AD-A122 866 THE NRL SOLRAD 11 SATELLITES (1976-023C 1976-023D) 1/1
DESCRIPTION OF EXPERIMENTS(U) NAVAL RESEARCH LAB
WASHINGTON DC D M HORAN ET AL. 30 NOV 82 NRL-MR-4959
UNCLASSIFIED SBI-AD-E000 516 F/G 22/1 NL

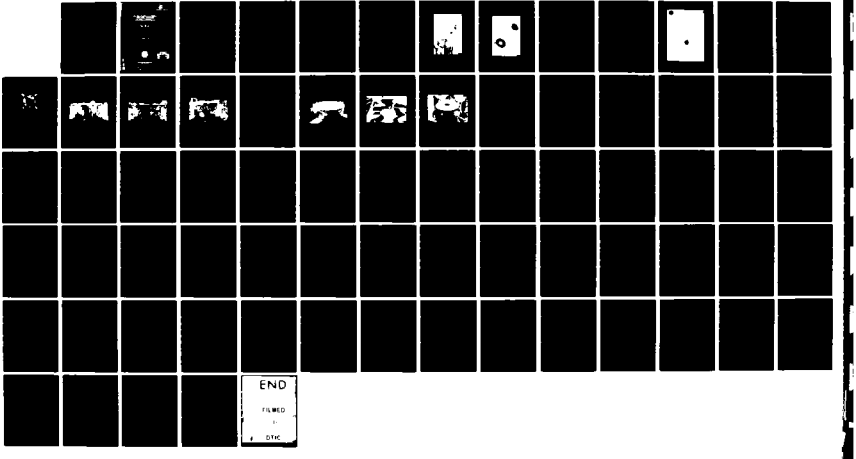

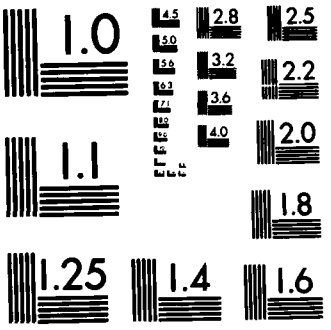

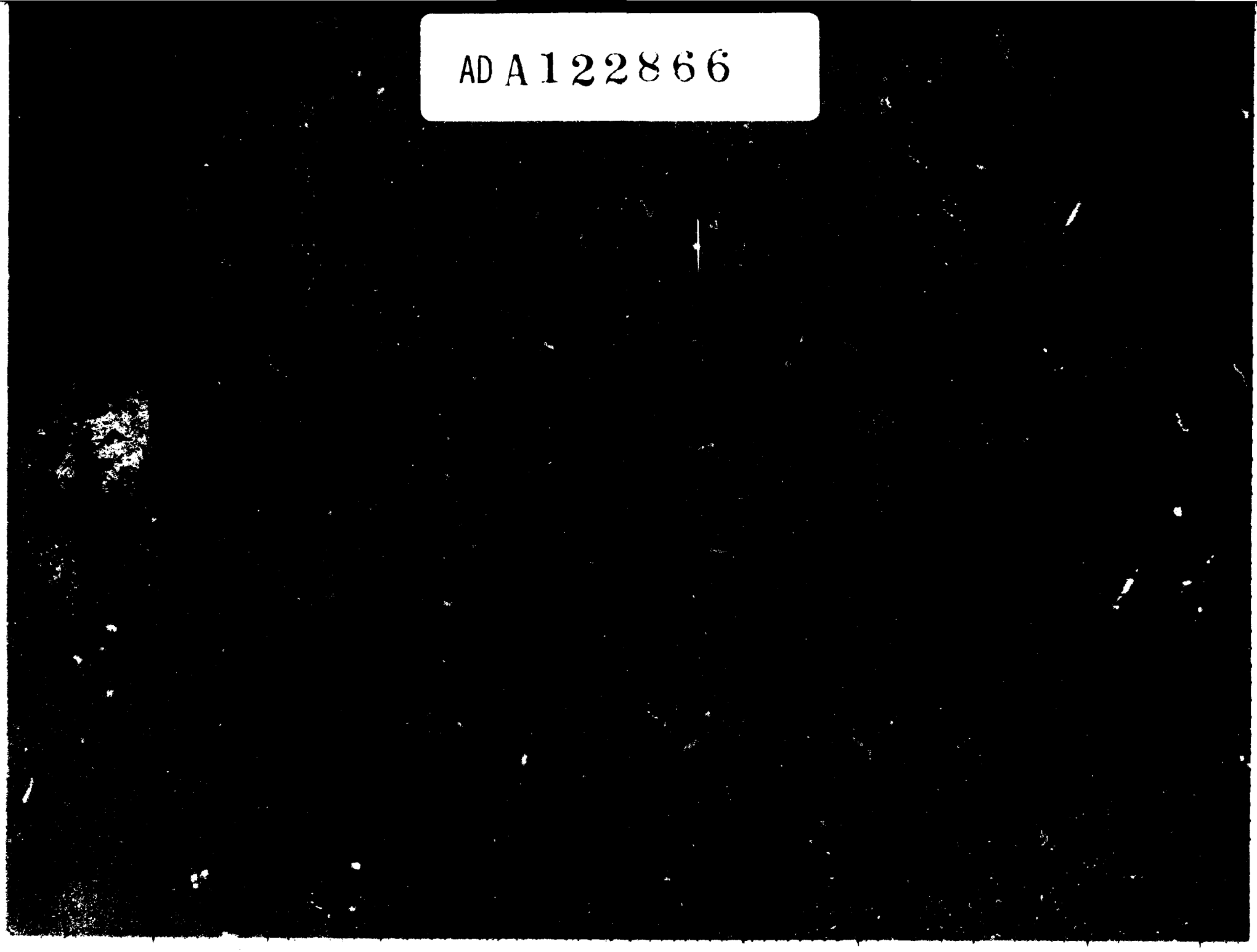

SECURITY CLASSIFICATION OF THIS PAGE (When Data Entered)

REPORT DOCUMENTATION PAGE		READ INSTRUCTIONS BEFORE COMPLETING FORM
1. REPORT NUMBER NRL Memorandum Report 4959	2. GOVT ACCESSION NO. A122 866	3. RECIPIENT'S CATALOG NUMBER
4. TITLE (and Subtitle) THE NRL SOLRAD 11 SATELLITES (1976-023C, 1976-023D) DESCRIPTION OF EXPERIMENTS		5. TYPE OF REPORT & PERIOD COVERED Final report on the NRL problem. 6. PERFORMING ORG. REPORT NUMBER
7. AUTHOR(s) D. M. Horan, R. W. Kreplin, and K. P. Dere		8. CONTRACT OR GRANT NUMBER(s)
9. PERFORMING ORGANIZATION NAME AND ADDRESS Naval Research Laboratory Washington, DC 20375		10. PROGRAM ELEMENT, PROJECT, TASK AREA & WORK UNIT NUMBERS 41-A01-20
11. CONTROLLING OFFICE NAME AND ADDRESS		12. REPORT DATE November 30, 1982 13. NUMBER OF PAGES 71
14. MONITORING AGENCY NAME & ADDRESS(if different from Controlling Office)		15. SECURITY CLASS. (of this report) UNCLASSIFIED 15a. DECLASSIFICATION/DOWNGRADING SCHEDULE

16. DISTRIBUTION STATEMENT (of this Report)

Approved for public release; distribution unlimited

17. DISTRIBUTION STATEMENT (of the abstract entered in Block 20, if different from Report)

18. SUPPLEMENTARY NOTES

19. KEY WORDS (Continue on reverse side if necessary and identify by block number)

SOLRAD satellites
SOLRAD 11
Solar monitoring

20. ABSTRACT (Continue on reverse side if necessary and identify by block number)

The Naval Research Laboratory's SOLRAD 11 satellites were successfully launched on 15 March 1976. The two satellites each carried an identical complement of 25 experiments to measure solar electromagnetic and charged particle emissions, Earth auroral and stellar X-ray emission, terrestrial and interplanetary extreme ultraviolet emission, X-ray and charged particle emission from the anti-solar direction, and gamma ray bursts. This report provides general descriptive information on the satellites and their sensors.

DD FORM 1 JAN 73 1473 EDITION OF 1 NOV 65 IS OBSOLETE
S/N 0102-014-6601

SECURITY CLASSIFICATION OF THIS PAGE (When Data Entered)

CONTENTS

GLOSSARY

A-D	Analog to digital
FPA	Floating point accumulator. See page 7.
FSP	Format start pulse. See page 5.
TMTC	Two minute telemetry cycle. See page 5.

The NRL SOLRAD 11 Satellites (1976-023C, 1976-023D)
Description of Experiments

INTRODUCTION

This document is intended to provide general, descriptive information on the SOLRAD 11 satellites and their sensors. Detailed information on the command, telemetry, control, and data sampling sequences for each experiment and on decoding the telemetry stream can be found in "SOLRAD 11 Experiment Timing, Telemetry and Command Summary" by D.M. Horan, R.W. Kreplin, K.P. Dere, and C.Y. Johnson, NRL Memorandum Report 3754, April 1978.

The Naval Research Laboratory's SOLRAD 11 satellites, 11A (1976-023C) and 11B (1976-023D) are the last of a series of ten successful satellites which began with the launch of SOLRAD 1 on 22 June 1960. Prior to SOLRAD 11, the SOLRAD satellites were designed to measure only solar electromagnetic radiation. The last seven satellites have been highly successful in obtaining useful x-ray data - SOLRAD 7A (1964-01D), SOLRAD 7B (1965-16D), SOLRAD 8 (1965-93A), SOLRAD 9 (1968-17A), SOLRAD 10 (1971-058A), and SOLRAD 11A and 11B.

The SOLRAD 11 satellites were successfully launched aboard a USAF Titan IIIC at 0125 UT on 15 March 1976. The Titan launch vehicle carried its payload to synchronous orbit and ejected the two SOLRAD 11 satellites and two small rockets as a unit. The small rockets were fired to raise the SOLRAD payload to a 120,000 km apogee and then to circularize the orbit at that altitude (Figure 1) with an inclination of approximately 6° to the ecliptic. The two SOLRAD satellites were separated on 22 March 1976 and moved slowly apart in their orbit until they reached a phasing of 180° in early July 1976.

Each satellite is washer shaped with an outside diameter of 58 inches, inside diameter of 24 inches, and a thickness of 16 inches (Figure 2). Four solar cell paddles extend like windmill blades and add 42 inches to the overall diameter. Lift off weight of each satellite was approximately 400 pounds. Each spacecraft carried an identical complement of 25 experiments to measure solar electromagnetic and charged particle emissions, Earth auroral and stellar x-ray emission, terrestrial and interplanetary extreme ultraviolet (EUV) emission, x-ray and charged particle emission from the anti-solar direction, and gamma ray bursts. A list of the experiments follows.

Manuscript submitted October 6, 1982.

Fig. 1 — Artist's concept of firing of small rocket to lift the SOLRAD 11 satellites from synchronous orbit toward final orbit at 20 Earth radii

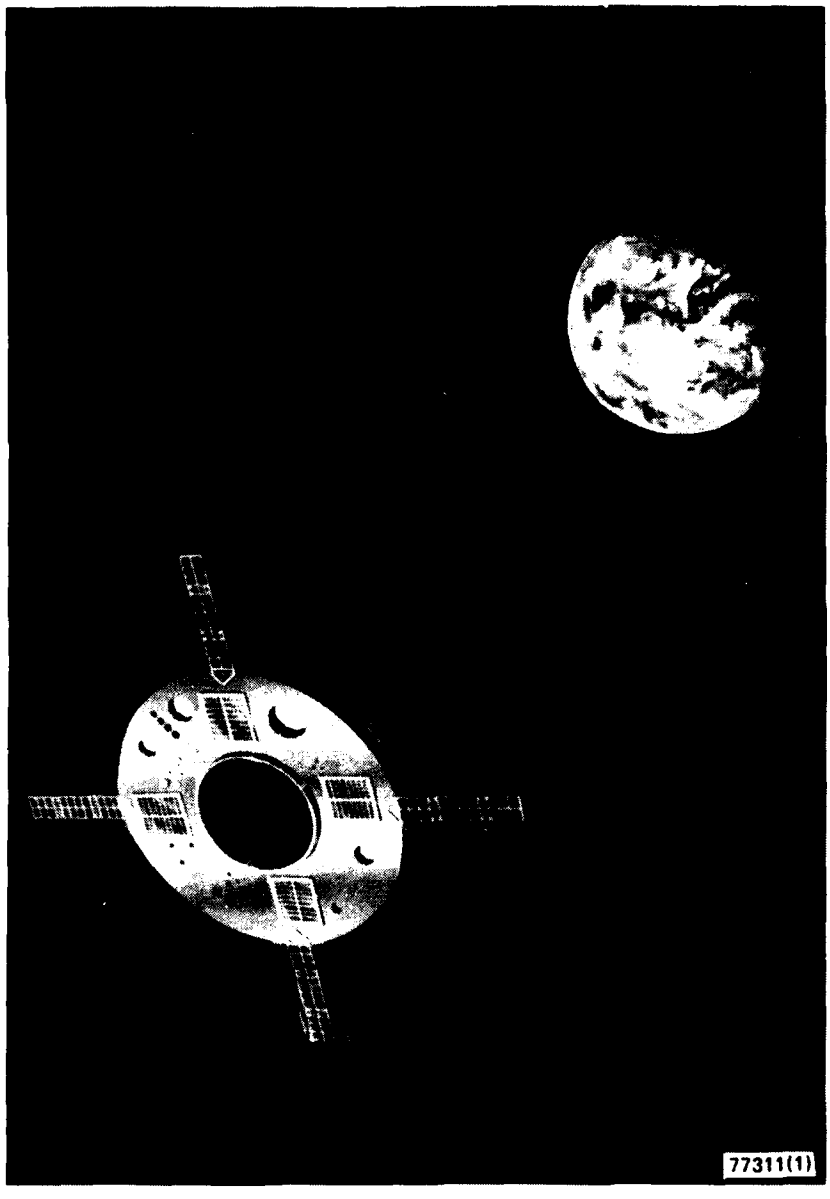

Fig. 2 — Artist's concept of one SOLRAD 11 satellite on station in circular orbit at 20 Earth radii

Experiment Number	Name
1	High Energy X-ray Monitor
2	X-ray Proportional Counter
3	Mg XI and Mg XII Line Monitor
4	1 to 8 Å Ionization Chamber
5	8 to 16 Å Ionization Chamber
6	44 to 60 Å Ionization Chamber
7	100 to 1030 Å - Three Bands
8	1080 to 1350 Å Ionization Chamber
9	Ultraviolet Spectrometer
10	Thomson X-ray Polarimeter
11	Bragg X-ray Polarimeter
12	0.5 to 3 Å Ionization Chamber
13	2 to 10 Å Ionization Chamber
14	Solar Protons > 10 Mev
15	Solar Wind
16	Stellar/Auroral X-rays
17	Omnidirectional Protons
18	Geocoronal - Extraterrestrial EUV
19	Geocoronal - Extraterrestrial EUV
20	Proton-alpha Telescope
21	Low Energy Proton Spectrometer
22	Solar Flare Electrons
23	Anti-Solar Protons > 10 Mev
24	X-ray Background
25	Gamma Ray Burst Monitor

The satellites were roll stabilized at 15 rpm with the roll axis pointing toward the Sun. Telemetry was continuous and in real time. Neither satellite carried data recording equipment.

The satellites are no longer operating. SOLRAD 11A suffered a failure in its telemetry system in June 1977. SOLRAD 11B was turned off in October 1979 when project funding was terminated.

SOLRAD HIGH CONCEPT

The launch of SOLRAD 11A and 11B implemented a concept called SOLRAD High. The original SOLRAD High concept called for three satellites phased 120° apart in a 20 Earth radii circular orbit with two widely separated ground stations. The satellites were to provide continuous real time solar measurements for use by the Naval Ocean Systems Command in their fleet support demonstrations and by the Air Force and the National Oceanic and Atmospheric Administration for their aerospace environment forecast center. The concept was reduced to a two satellite configuraion when an opportunity to launch two satellies, but not three, presented itself. Since continuous real time data could be achieved using two satellites and two ground stations, it was decided that the opportunity for a two satellite launch should be seized rather than wait an unknown

period of time for a three satellite launch opportunity. The second ground station was never stricken from the concept. However, it was effectively eliminated because funds were never provided for it.

The concept, as implemented, consists of two satellites phased 180° apart in a 20 Earth radii circular orbit with a single ground station at Blossom Point, Maryland near Washington, D.C. (Figure 3). Since the satellites had an orbital period of approximately 120 hours, passage of a satellite over the ground station was governed more by the Earth's rotation than by the motion of the satellite. Therefore, a single pass of a SOLRAD 11 satellite over the ground station lasted several hours, and in fact ranged between 9 and 18 hours because of the inclination of the orbit.

SATELLITE SYSTEMS

Several satellite systems are directly tied to the operation of the experiments and it is useful to discuss them before describing the experiments. Therefore, in this section we will describe the telemetry system, the solar aspect system, and the roll reference system.

Telemetry System

Each SOLRAD 11 satellite has a single digital, real time telemetry link to carry all experiment and housekeeping data. There are five telemetry formats. Each consists of 32 frames containing 32 twelve-bit words. The information rate is 102.4 bits per second. It requires 3.75 seconds to transmit one frame and two minutes to transmit one format page of 32 frames. One format page is defined by a complete cycle of the five least significant bits of the ten bit frame identification counter and is one of the basic time intervals of the satellites. At the beginning of the frame in which these five least significant bits change from all one state to all zero state a pulse called the format start pulse (FSP) is generated and communicated throughout the satellite. The FSP triggers many operations in the experiments, including commencement and termination of data acquisition or calibration cycles. Many commands to the satellites are not executed until the first FSP after reception of the command. The telemetry frame for which the five least significant bits of the frame identification counter are all in zero state is called "frame zero". The two minute interval between FSP's is called a two minute telemetry cycle (TMTC).

Each of the five telemetry formats carries a different set of data. Format one, which is normally selected, contains data from all experiments except 18, 19, and 25. Format two replaces some data from experiments 4, 5, 12, and 13 with data from experiments 18, 19, and 25. Experiments 18 and 19 were excluded from format one because these experiments are normally turned off. Experiment 25 was excluded because it has a memory and does not require continuous transmission. Format two is normally selected for about two hours

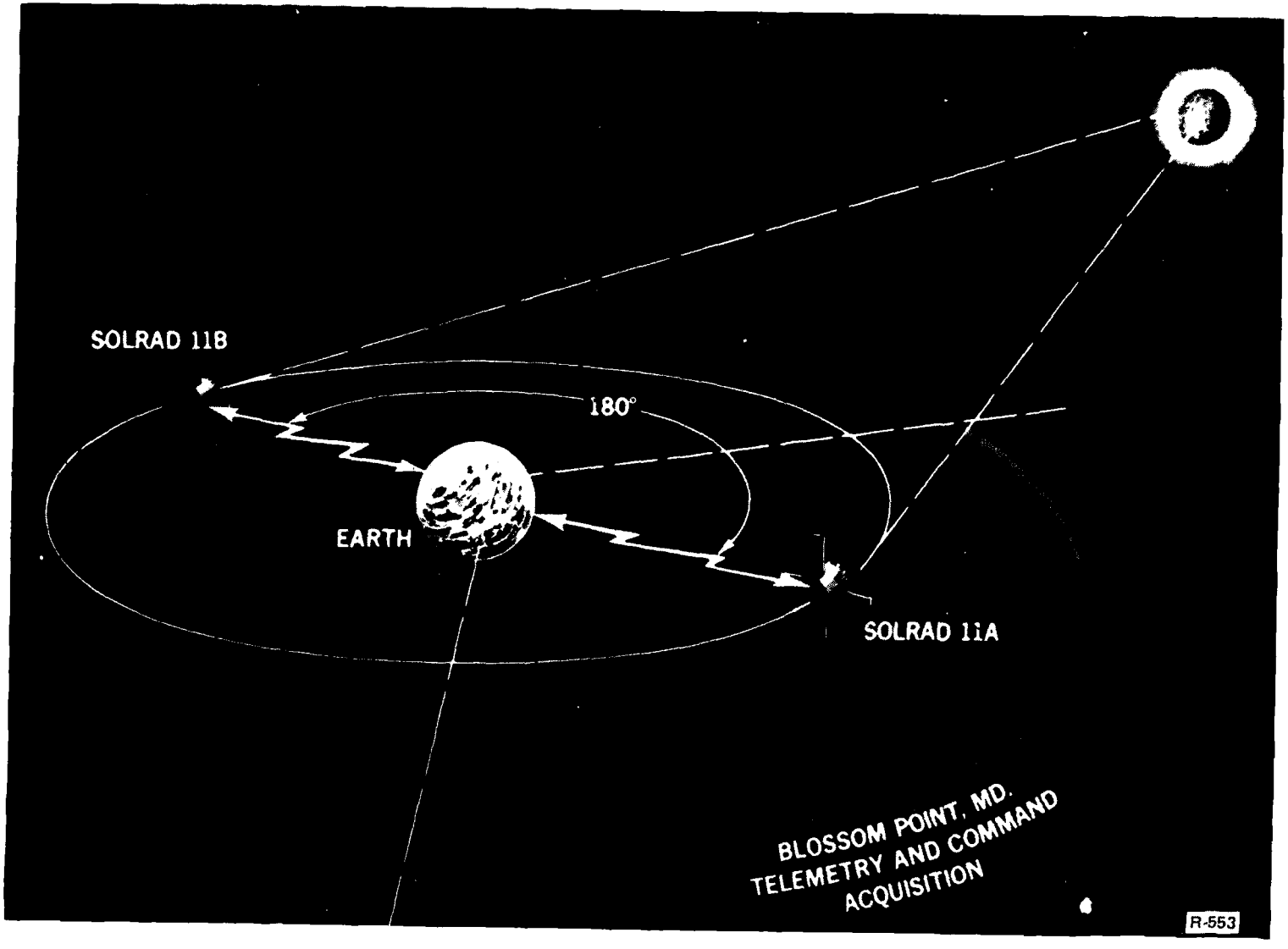

Fig. 3 — SOLRAD High concept as flown with two satellites phased 180° apart in a 20 Earth radii (80,000 mile) circular orbit and one ground station for telemetry acquisition and command

per day. Format three devotes about two-thirds of the telemetry capability to experiment 15. It is used infrequently and for short time intervals because it excludes data from most of the other experiments. Format four is primarily devoted to housekeeping and status information. It is used to obtain a rapid check on the condition of the satellite and the experiments. Very little experiment data is contained in format four. Format five provides satellite orientation information with very high time resolution. It is only used when modifying the orbit.

Data and information are encoded into the twelve-bit telemetry words in several ways. Analog data is converted to digital form, usually with eight bit resolution but in some cases with twelve bit resolution. Digital data is sometimes encoded directly from linear accumulators. More often the digital data from the experiments is encoded by letting the telemetry words carry the output of a twelve-bit floating point accumulator (FPA). The FPA information is carried in the form of a four-bit exponent and an eight-bit mantissa. An FPA has a range from 0 to 16 million counts with a resolution better than 0.5% over the entire range.

Solar Aspect System

The SOLRAD 11 satellites are roll stabilized with the roll axis normally aligned toward the Sun and the roll rate maintained near 15 revolutions per minute. The solar aspect system measures the angle between the satellite's roll axis and the satellite-Sun line, the solar aspect angle, and generates a solar pulse which permits calculation of the location of the Sun projected on a plane perpendicular to the roll axis. Each satellite has wide angle and fine angle solar aspect sensors. The wide angle sensors are used when the solar aspect angle exceeds 5°; the fine angle sensors are used for smaller solar aspect angles.

The solar aspect angle is maintained between 0.5 and 1.0 degree for optimium performance of the solar oriented experiments and fuel conservation. The solar aspect angle must frequently be corrected because the motion of the Earth in its orbit causes the solar aspect angle to change by nearly 1° per day. This correction is done automatically based on measurements by the solar aspect sensors. Telemetered information from the solar aspect sensors permits precise calculation of the orientation in space of the roll axis.

As the satellite rolls about its axis with a nonzero solar aspect angle, the Sun's image traces a circle on a plane perpendicular to the roll axis. Once each revoluton, when the Sun has a certain angular offset with respect to a solar aspect sensor, the solar aspect system triggers a solar pulse within the satellite. This solar pulse then starts or stops timers within the satellite's roll reference system. Telemetered values from these timers can be used to calculate the precise roll rate and the orientation of the roll plane on the celestial sphere. The solar pulse can be used by the roll reference system to generate star and Earth pulses to control

data acquisition sequences for various experiments.

Roll Reference System

The roll reference system generates a star pulse and an Earth pulse as reference points for electronic sectoring of the roll plane for experiment data acquisition. The star or Earth pulse can be caused by passage of the Earth through the fan shaped field of view of infrared or visible light Earth sensor arrays, or by the solar pulse generated by the solar aspect system. The star or Earth pulses were also to be caused by detection of the star Canopus by a stellar sensor, but this system failed to lock on Canopus. The roll reference system contains programmable time delays which can be set to selected levels by command from the ground station. Use of the programmable time delays permits the generation of the star or Earth pulse to be delayed, rather than simultaneous with the sensing of the target by the selected Earth or solar sensor. Electronic gates are also set by ground command to select the sensor to be used as the source of the star and/or Earth pulse.

The star and Earth pulses control the division of the roll plane into 64 sectors and gating of experiment data into accumulators associated with the sectors. The time of generation of the star pulse marks the beginning of the first of the 64 sectors. The direction in which a given experiment sensor is looking when the star pulse is generated marks the origin of the 64 sectors for that particular experiment sensor. Therefore, the orientation of the roll plane sector boundaries for a given experiment sensor is a function of the sensor chosen as source of the star or Earth pulse by the electronic gate settings, the values put into the programmable time delays, and the location of the experiment sensor on the satellite.

The star and Earth pulses also start and stop timers in the roll reference system. These timers are also affected by the solar pulse and the frame start pulse (FSP). Data telemetered from these timers can be used to calculate the roll period, orient the roll plane sector boundaries for each experiment sensor, calculate the orientation of the roll axis, and synchronize data acquisition with the telemetry frames.

DESCRIPTION OF EXPERIMENTS

Most of the experiment sensors are located on, or under, the solar oriented surface of each satellite. These include the sensors for experiments 1 through 14 and the positive ion cup for experiment 15. The electron cup for experiment 15 and the sensors for experiments 17 through 22 are all mounted on the sides of the satellites. The sensors for experiments 23 and 24 are mounted on the anti-solar surface of each satellite. Figure 4a is a photograph of the solar oriented surface of a SOLRAD 11 satellite with a line drawing indicating the location of the experiment sensors or their apertures. Figures 4b, 4c, and 4d are photographs showing the

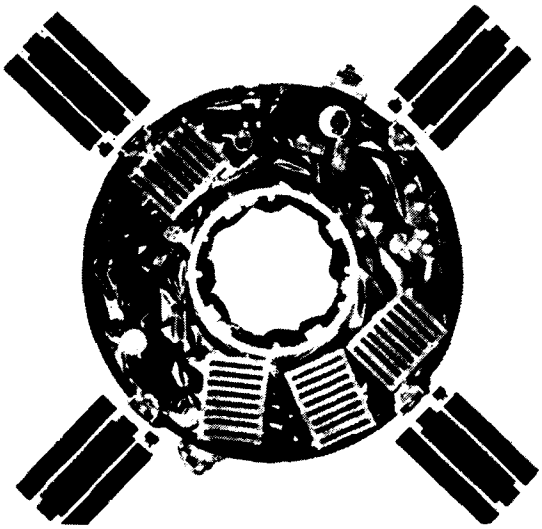

R-558

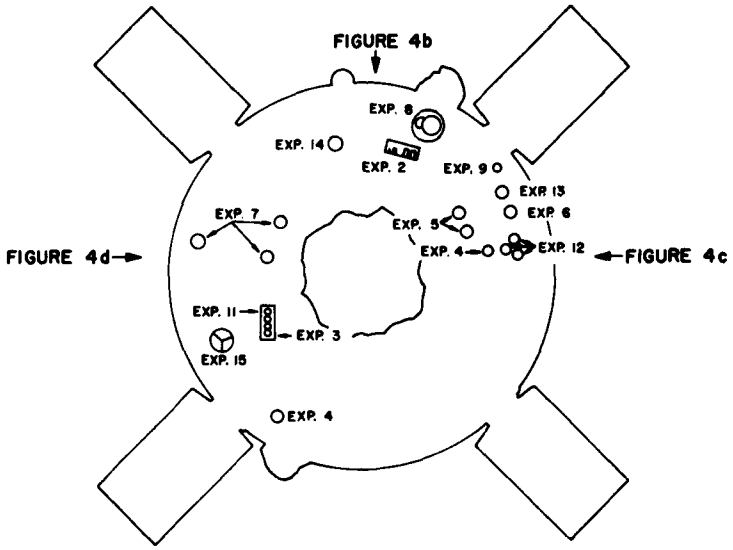

Fig. 4a — Photograph of solar oriented surface of SOLRAD 11 satellite with line drawing indicating location of experiment sensors or apertures. The fields of view of Figures 4b, 4c, and 4d are indicated by arrows

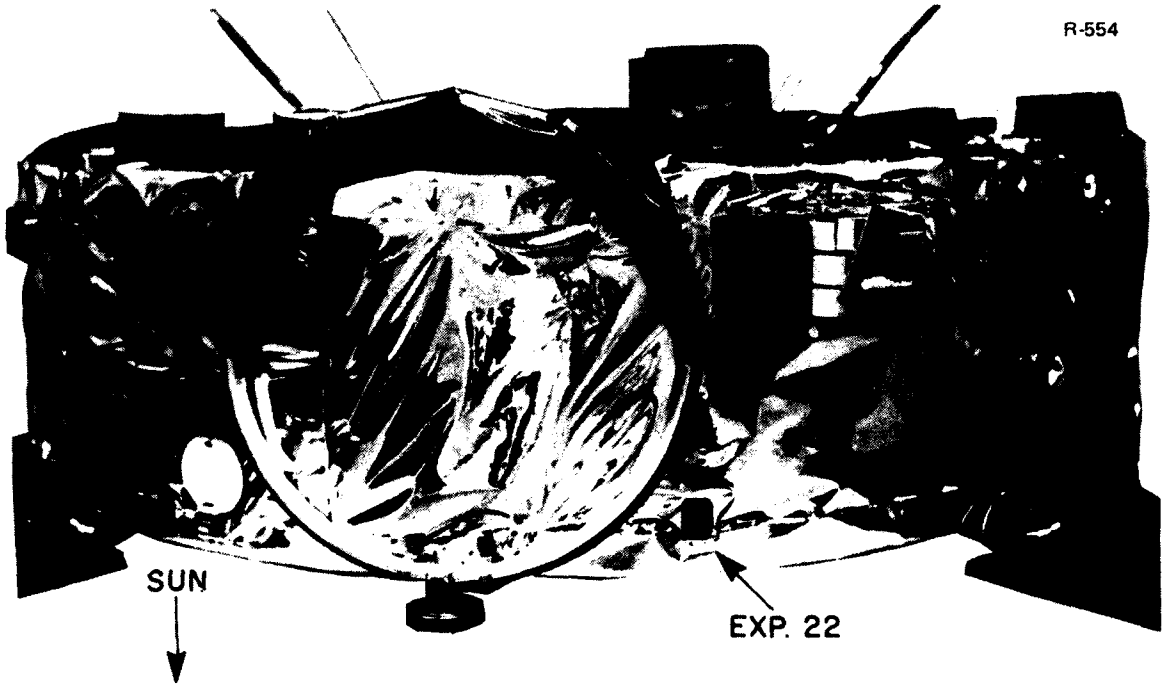

Fig. 4b — Photograph of side of SOLRAD 11A satellite indicating location of sensors or apertures for side-mounted experiments. Orientation can be obtained from Figure 4a.

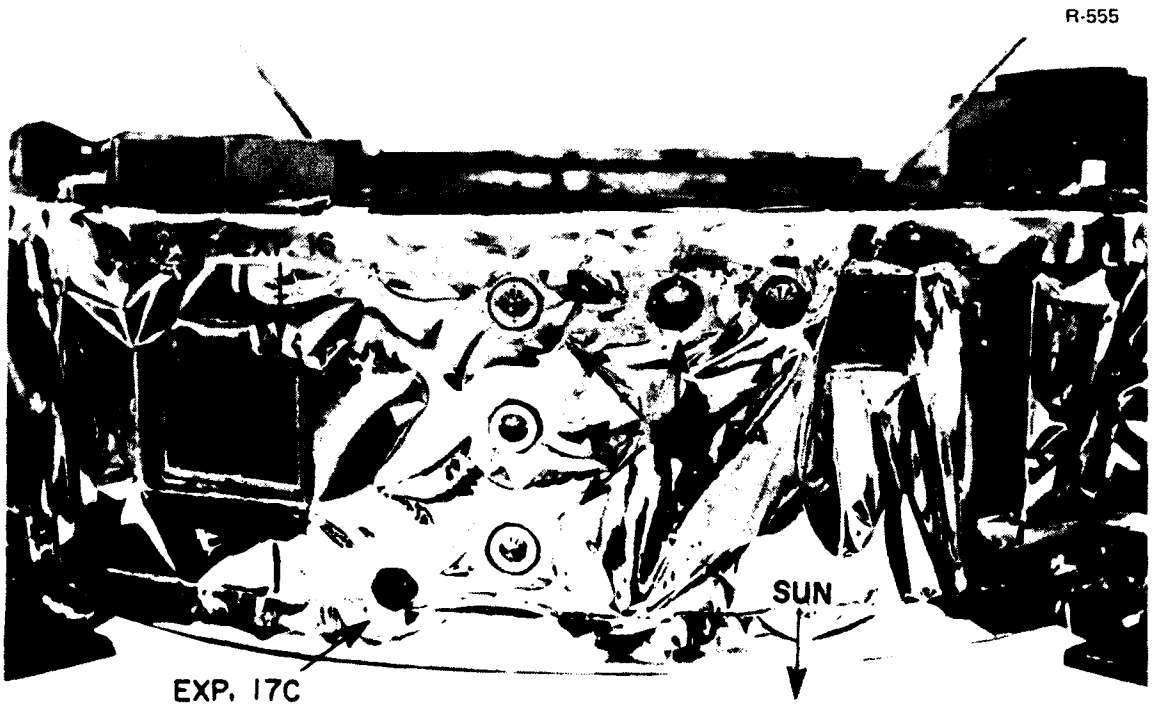

Fig. 4c — Photograph of side of SOLRAD 11A satellite indicating location of sensors or apertures for side-mounted experiments. Orientation can be obtained from Figure 4a.

Fig. 4d — Photograph of side of SOLRAD 11A satellite indicate location of sensors or apertures for side-mounted experiments. Orientation can be obtained from Figure 4a.

sensors and apertures for the experiments mounted on the sides of the satellites. The directions from which the photographs in Figures 4b - 4d were taken are indicated on Figure 4a. Figure 4e is a photograph of the anti-solar surface of a SOLRAD 11 satellite. Experiments 23 and 24 are under covers which protected them during the ascent to orbit. Figure 4f and 4g show the aperture for experiment 23 and experiment 24, respectively. Experiments 1, 10, and 25 are mounted inside and have no apertures in the surface of the satellites.

Experiment 1, High Energy X-ray Monitor:

Experimenter: G.G. Fritz, Code 4120, Naval Research Laboratory

This experiment is intended to measure the flux of hard x-rays which are generally seen only during solar flares. A 1 cm thick sodium doped CsI scintillating crystal surrounded by a plastic scintillating material is used to detect solar x-rays with energy between 15 and 150 kev. A single photomultiplier detects light bursts in the CsI or plastic. Electronic rise time discrimination is used to separate the fast, particle-induced bursts in the plastic from the slower bursts produced in the CsI by x-rays and particles. Bursts generated by x-rays are subjected to pulse height analysis for separation into four energy ranges:

15-20 kev	Channel 1
20-30 kev	Channel 2
30-60 kev	Channel 3
60-150 kev	Channel 4

The scintillator has a 10 cm^2 effective area. Normally pulses from all four energy ranges are accumulated in four FPA's during the same 7.50 second sampling interval and their values telemetered during the next sampling interval. The experiment can be commanded into an optional sampling mode in which pulses from the 20-30 kev energy range, channel 2, accumulate for 1.875 seconds and their total count is telemetered during the next 1.875 second period. No information from channels 1, 3, and 4 is collected in this optional sampling mode.

In-flight adjustment of the energy channel bounds is achieved by use of an Am 241 source of 60 kev x-rays and high voltage power supplies which can be commanded to 16 output levels. The experiment has two high voltage power supplies for redundancy. When the calibration sequence is commanded the radioactive source swings in front of the detector at the beginning of the next telemetry cycle, remains there for the entire two minute cycle, and then swings back into its shielded enclosure. The calibration sequence can also be terminated at any time by a separate command. Changes

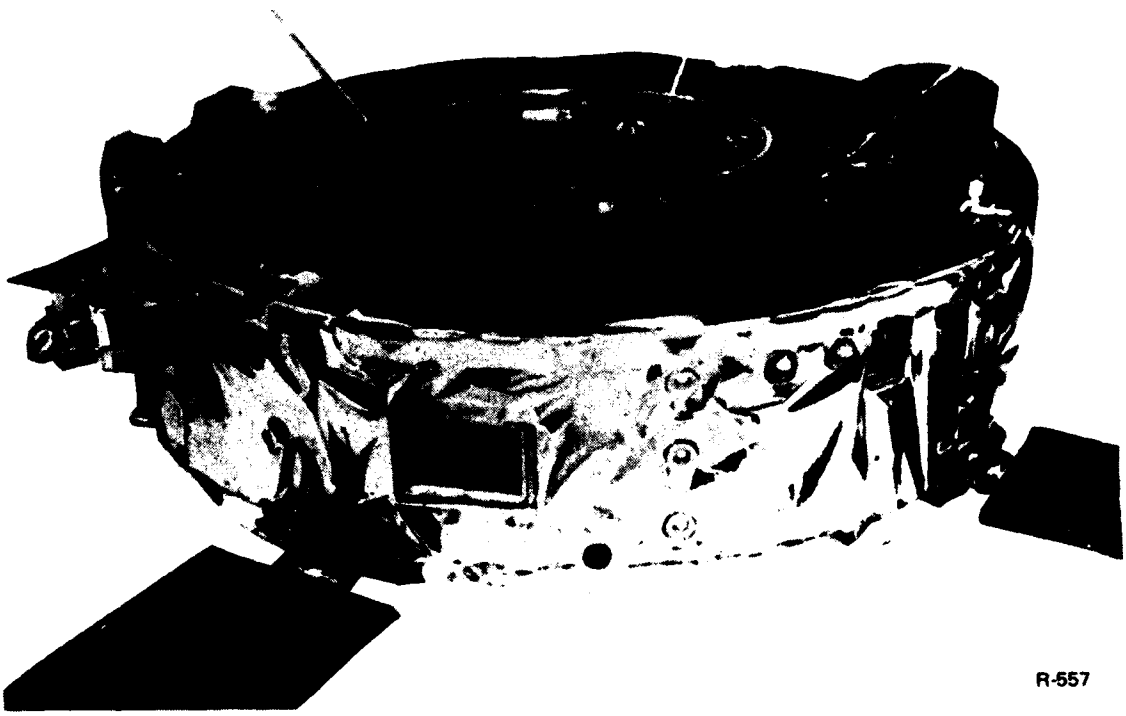

Fig. 4e — Photograph of anti-solar surface of SOLRAD 11A satellite showing protective covers over experiments 23 and 24.

Fig. 4f — Photograph of aperture of experiment 23 on anti-solar surface of SOLRAD 11A

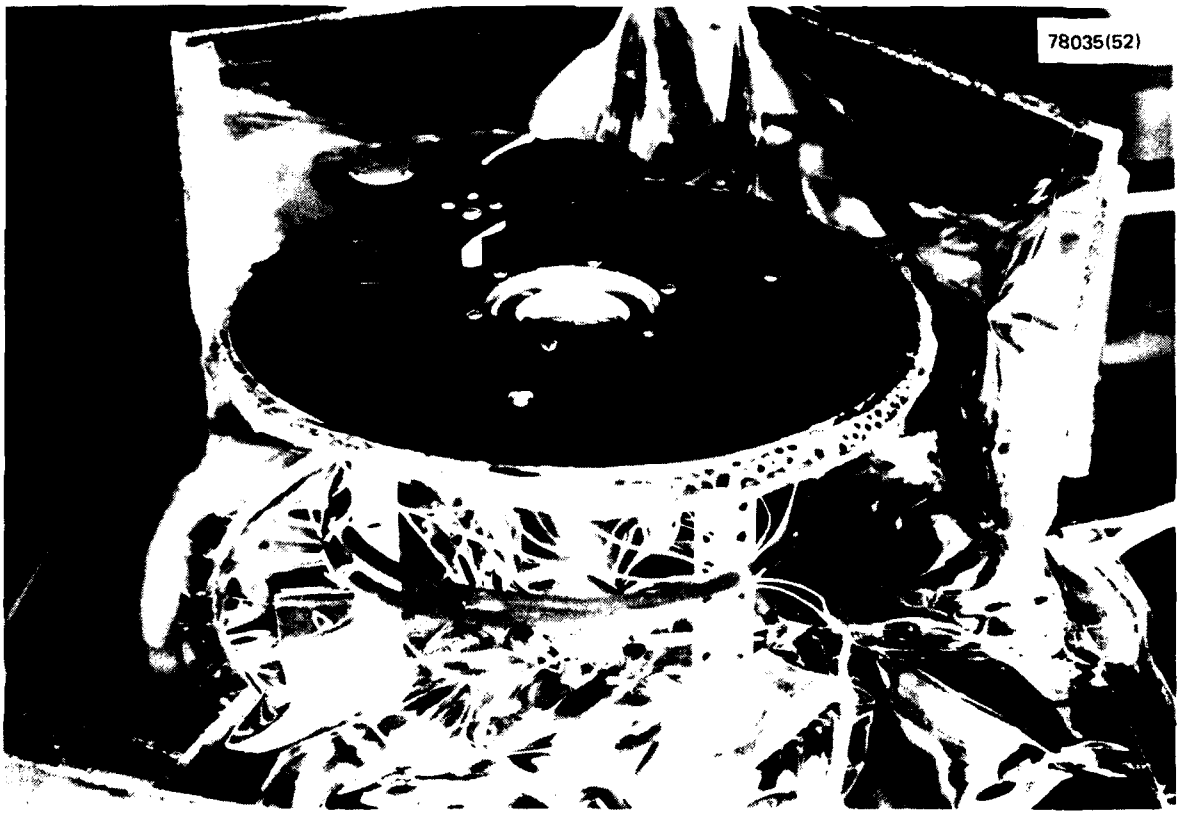

Fig. 4g — Photograph of experiment 24 on anti-solar surface of SOLRAD 11 satellite

in the photomultiplier gain are offset by adjusting the high voltage output level until the counts in channels 3 and 4 from the 60 kev x-ray source are most nearly equal.

A ratemeter monitors the pulse rate in the plastic scintillator as a measure of the false counts generated in the CsI by charged particles. The 0 to 5 volt analog output of the ratemeter is sampled at one minute intervals, subjected to 8-bit A-D conversion, and telemetered within a few milliseconds of taking the sample.

Figure 5 shows the efficiency of the experiment as a function of energy over the 10 to 150 kev band. The low energy sensitivity is determined by a 0.020 inch thick aluminum window.

Experiment 2, X-ray Proportional Counter:

Experimenter: H.W. Smathers, Jr., Code 4120, Naval Research Laboratory

This experiment is intended to measure solar x-rays in a range of energies overlapping and extending that of the 0.5 to 3 Å ionization chamber. Four gas filled proportional counters are used to detect solar x-rays with energy between 3 and 60 kev. The proportional counters are paired so that two counters share the same gas filling but have separate entrance windows and independent pulse counting electronics. The 3 to 7.5 and 7.5 to 15 kev counters are paired and have a gas filling of 70% Ne and 30% CO_2 at 2 atmospheres pressure. The 15 to 30 and 30 to 60 kev counters share a gas filling of 90% Kr and 10% CO_2 at 152 mm Hg. Electronic pulse height discrimination limits counting to the desired x-ray energy range for each counter.

Energy Range	Gas	Window Area
3.0-7.5 kev	Ne-CO_2	0.010 cm^2
7.5-15 kev	Ne-CO_2	0.100 cm^2
15-30 kev	Kr-CO_2	0.200 cm^2
30-60 kev	Kr-CO_2	0.200 cm^2

Normally pulses from all four counters are accumulated in four FPA's during the same 7.50 second sampling interval and their values telemetered during the next sampling interval. The experiment can be commanded into two optional sampling modes. In one optional mode pulses from any two of the counters are accumulated for 3.750 seconds and their values telemetered during the next 3.750 second interval. In the other optional mode pulses from any one of the counters are accumulated for 1.875 seconds and the value telemetered during the next 1.875 second interval. The assocation of specific counters with specific FPA's is completely interchangeable by command. This interchangeability permits selection of the specific counters to be sampled and telemetered in the two optional modes. However it also means that the order in which data is read out from four or two channels is not constant and must be determined from telemetered

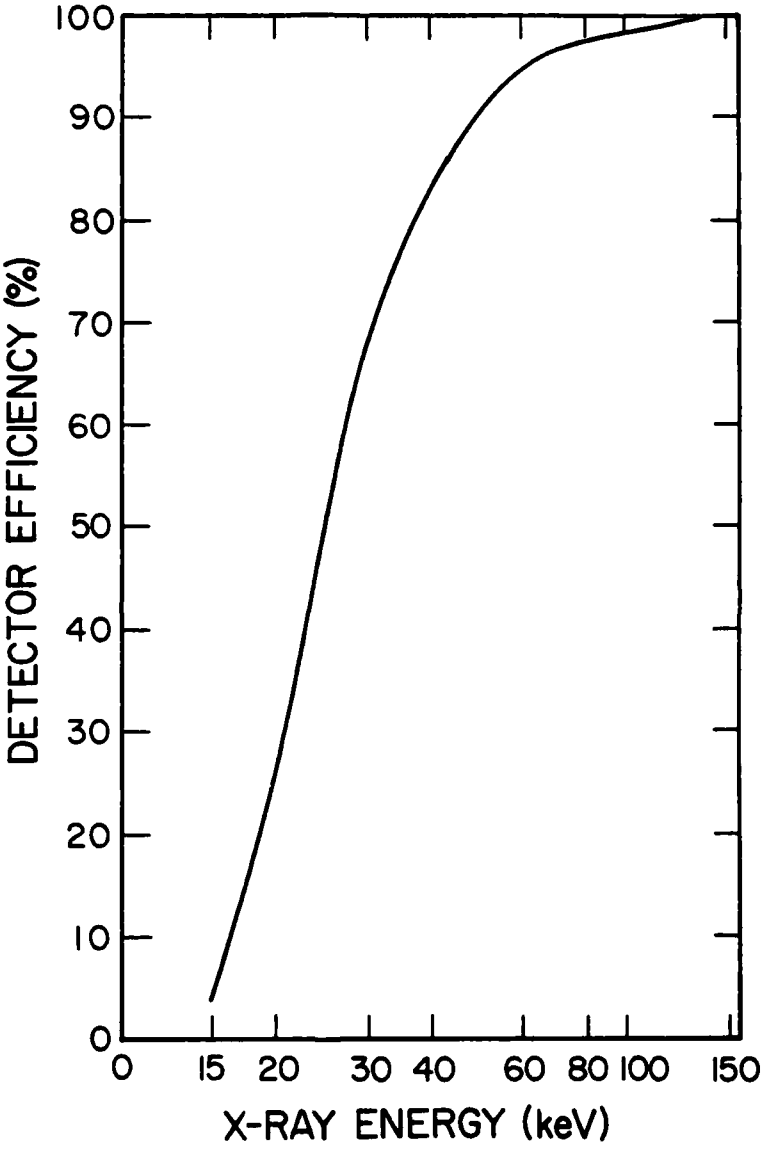

Fig. 5 — Efficiency of experiment 1 hard x-ray detectors as a function of x-ray energy

status information.

In-flight adjustment of the energy channel bounds is achieved by use of Fe 55 and Cd 109 radioactive sources and high voltage power supplies which can be commanded to 16 output levels. The Fe 55 is used with the neon filled unit and the Cd 109 is used with the krypton filled unit. Prior to exposing a radioactive source, a command replaces accumulation of the normal deep counter pulse count with a pulse count determined by a second set of discriminator settings for the shallow counter. When a calibration sequence is commanded, the appropriate radioactive source swings in front of the shallow counter's window at the beginning of the next telemetry cycle, remains there for the entire two minutes, and then swings back into its shielded enclosure. The source exposure can also be terminated at any time by a separate command. Changes in the proportional counter gain are offset by adjusting the high voltage output level until the counts generated in the normal shallow counter band by a radioactive source are approximately twice those in the special shallow counter band. Each counter pair is driven by a single high voltage power supply, but four high voltage power supplies are contained in the experiment for redundancy.

Experiment 3, Mg XI and Mg XII Line Monitor:

Experimenter: J.F. Meekins, Code 4120, Naval Research Laboratory

This experiment is intended to measure x-ray emission line intensity from hydrogen-like and helium-like magnesium ions which may provide an indication of temperature changes in the solar corona. The helium-like Mg XI dominance is indicative of plasma at about 4×10^6 K while the hydrogen-like Mg XII is dominant in 7×10^6 K plasmas. Changes in the ratio of line emission intensities indicate changing temperatures in the coronal plasma.

Three ADP (ammonium dihydrogen phosphate) crystals are fixed at three different angles to allow x-rays of 9.17 Å, 8.42 Å, and 8.80 Å to undergo first order Bragg reflection into three proportional counters. The crystals are fixed with reference to the satellite's calculated roll axis and assume perfect alignment of the roll axis and the satellite-Sun line. However, the crystal material was selected to permit proper operation even if the roll axis is pointing as much as 1° from the source region on the Sun. If the roll axis is not pointing directly at the solar source region the experiment functions as a scanning spectrometer with extremely limited spectral range in the vicinity of the target wavelengths. The line emission at 9.17 Å (Mg XI) and 8.42 Å (Mg XII) causes the highest counting rates over the scanning ranges of their crystals. The spacecraft's roll reference system generates pulses at intervals of 1/64th of the roll period which bound count accumulation periods for the three proportional counters. Electronic comparators within the experiment

identify and store the largest of the 64 accumulations during a roll period from each of the two crystals aligned for line emission. The accumulator counting 8.80 Å continuum pulses is slaved to one of the line emission crystals so that the continuum sample simultaneous with the saved line emission sample is also saved. The relationship of the fixed angles of the crystals is such that when the line emission crystals are reflecting their target lines, the continuum crystal is reflecting continuum emission. When the spacecraft's roll reference system indicates the end of each roll period by generating a star pulse, the saved values for the three accumulators plus one count are added to values contained in adder registers. At the midpoint and end of each TMTC the values in the three adder registers are shifted into storage registers for telemetering during the next minute and the adder registers are set to zero. The x-ray line emission is obtained from telemetered values as follows:

$$F = \frac{[\ L - C\ ]}{a\ T} \qquad (1)$$

where F is the line emission in photons/cm^2 sec;
L is the telemetered digital value for the line emission;
C is the telemetered digital value for the continuum emission;
T is the data accumulation interval in seconds;
a is a constant based on aperture, crystal reflectivity, transmittance of the Mylar window, and counter efficiency.

The data accumulation interval is approximately equal to N/64 times the roll period, where N is the number of star pulses during the half of the TMTC associated with the data accumulation. The value of the constant a is:

Line	a (cm^2)
8.42 Å	7.0×10^{-6}
9.17 Å	8.3×10^{-6}

The experiment contains two high voltage power supplies for redundancy although the three proportional counters are driven by a single supply. The power supplies can be independently commanded to 16 output levels.

Experiment 4, 1 to 8 Å Ionization Chamber:

Experimenters: R.W. Kreplin, D.M. Horan, K.P. Dere, R.G. Taylor, Code 4170, Naval Research Laboratory

This experiment uses ionization chambers to measure solar emission over the 1 to 8 Å x-ray band. All of the SOLRAD

series satellites, starting with SOLRAD 1 in 1960, have carried 1 to 8 Å ionization chamber experiments and this extended monitoring effort has shown the 1 to 8 Å band to be significant for several reasons. At present it is the highest energy band that has been monitored through an entire eleven year solar cycle using simple, long-lived, stable sensors. The 1 to 8 Å emission from the quiet Sun varies by two orders of magnitude in phase with the solar cycle and can be used to trace progress through a solar cycle and to help define occurrence of solar maximum and minimum. Short term increases of two or three orders of magnitude above the quiet Sun level and lasting several minutes to an hour mark the occurrence of solar flares. The increased 1 to 8 Å emission has been widely used as a standard measure of flare size (Baker, 1970). In addition to its individual significance, the 1 to 8 Å measurements during solar flares can be analyzed with measurements from experiments 5, 12, and 13 to calculate a temperature and emission measure profile of the flaring plasma (Dere, et al., 1974) and to provide a reasonably accurate solar emission spectrum over the 1 to 20 Å band.

For redundancy the experiment is made up of two complete units designated 4A and 4B. Each unit consists of an ionization chamber sensitive to 1 to 8 Å x-rays and a four-range electrometer-amplifier. The units are connected to different power supplies. Only one unit at a time, selectable by command, is connected to telemetry. The 0 to 5 volt analog output of the selected unit, representing an instantaneous measurement of the current generated in the ionization chamber, is subjected to 8-bit A-D conversion and telemetered within a few milliseconds of taking the sample. The time interval between samples depends on the telemetry format, and is 7.5 seconds in formats 1, 3, and 4 and 15.0 seconds in format 2. A manual or automatic range changing mode of operation is selectable by command. In the automatic mode the magnitude of the output current from the ionization chamber is used to select the amplifier range. In manual mode the amplifier range is selected by command.

The experiment can be commanded into a calibration sequence that will measure drift in the quiescient (zero input current) level of the higher amplifier ranges. The ionization chamber is not disconnected from the amplifier so the calibration is most meaningful when the current generated in the ionization chamber is very small. If the experiment is in automatic range change mode when the calibration sequence is commanded, the amplifier will be switched to the most sensitive range, range 1, at the beginning of the next TMTC and the current in a calibration resistor will be measured. At thirty second intervals the amplifier will be switched to less sensitive ranges and the calibration sequence will terminate automatically at the end of the TMTC. If the experiment is in manual range change mode, the amplifier

will remain in the selected range for the entire two minutes. The calibration sequence can be terminated at any time by a separate command. Calibration sequences for experiments 4, 5, 6, 7, 8, 12, and 13 are initiated and terminated by the same commands and must occur simultaneously.

The current generated in an ionization chamber by incident solar radiation is given by

$$I = A\int_0^\infty R(\lambda)\, E(\lambda)\, d\lambda \qquad (2)$$

with

$$R(\lambda) = e\omega\varepsilon(\lambda)$$

where e is the electronic charge, ω is the number of ion pairs produced in the gas per unit energy of the incident photon, A is the effective window area of the detector, $E(\lambda)$ is the solar emission spectrum, $\varepsilon(\lambda)$ is the efficiency of the detector, and λ is the wavelength. The relationship between the energy flux (ergs/cm^2/sec) striking the window in a wavelength band defined by λ_a and λ_b and the current generated in the ionization chamber is given by

$$\frac{F(\lambda_a, \lambda_b)}{I} = \frac{\int_{\lambda_a}^{\lambda_b} E(\lambda)\, d\lambda}{e\omega A\int_0^\infty E(\lambda)\, \varepsilon(\lambda) d\lambda} = \frac{K(\lambda_a, \lambda_b)}{A} \qquad (3)$$

where K is a conversion coefficient which depends on the characteristics of the detector and the wavelength band of interest. In the case of SOLRAD 10 and earlier satellites, the value of K was calculated using an assumed solar emission spectrum, published values for ω, and calculated values for $\varepsilon(\lambda)$ based on mass absorption coefficients from many sources and average area densities, ρx (Horan and Kreplin, 1972). For SOLRAD 11 the values for K are based on direct measurements of the ionization chamber parameter $R(\lambda)$ at several wavelengths over the sensitive band followed by a curve fitting to obtain the values for ω and effective area densities which best duplicate the measured values (Meekins, et al., 1974). Table 1 gives the resulting values for K, A, ω and ρx along with other information describing the 1 to 8 Å sensors and Figure 6 gives the fitted curve for $R(\lambda)/e\omega$ which is equivalent to $\varepsilon(\lambda)$. Although a temperature dependent solar emission spectrum could be used, for reasons of simplicity, ease of conversion to any other spectral assumption, and continuity of a common basis with data from earlier SOLRAD satellites dating to 1960, the gray-body solar emission spectrum with a 2×10^6 K color temperature is assumed for SOLRAD 11 1 to 8 Å experiments (Kreplin, 1961; Horan and Kreplin, 1972).

The telemetered data is actually a measure of the output

Table 1

X-ray Sensor Values

Experiment	4	5	6	12	13
Band (Å)	1-8	8-20	44-60	0.5-3	2-10
Window Material: x(W) (g/cm^2)	Be: 2.82(-2) Al: 4.10(-5) Ar: 3.82(-4)	Al: 2.80(-3) N_2: 1.35(-5)	Mylar: 9.4(-4) N_2: 6.6(-5)	Be: 3.14(-1) Al: 4.10(-5) Kr: 1.61(-3)	Be: 9.57(-3) Al: 2.70(-5) Ne: 5.32(-5)
Gas: x(G) (g/cm^2)	Ar: 5.88(-3)	N_2: 1.238(-3)	N_2: 6.1(-4)	Kr: 2.48(-2)	Ne: 1.50(-3)
Sat: Exp: (ion pairs/erg)	11A:4A: 2.38(10) 11A:4B: 2.33(10) 11B:4A: 2.38(10) 11B:4B: 1.95(10)	11A:5A: 1.71(10) 11A:5B: 1.80(10) 11B:5A: 1.71(10) 11B:5B: 1.70(10)	11A: 1.80(10) 11B: 1.80(10)	11A: 2.57(10) 11B: 2.22(10)	11A: 1.71(10) 11B: 1.71(10)
Area (cm^2)	4.75	2.09	11A: 0.121 11B: 0.128	15.8	4.75
Sat: Exp: K (ergs/sec amp)	11A:4A: 5.67(9) 11B:4B: 5.79(9) 11B:4A: 5.67(9) 11B:4B: 6.92(9)	11A:5A: 8.81(9) 11A:5B: 8.37(9) 11B:5A: 8.81(9) 11B:5B: 8.86(9)	11A: 3.42(10) 11B: 3.42(10)	11A: 9.61(8) 11B: 1.11(9)	11A: 2.33(9) 11B: 2.33(9)

Key: 7.32(-5) = 7.32×10^{-5}

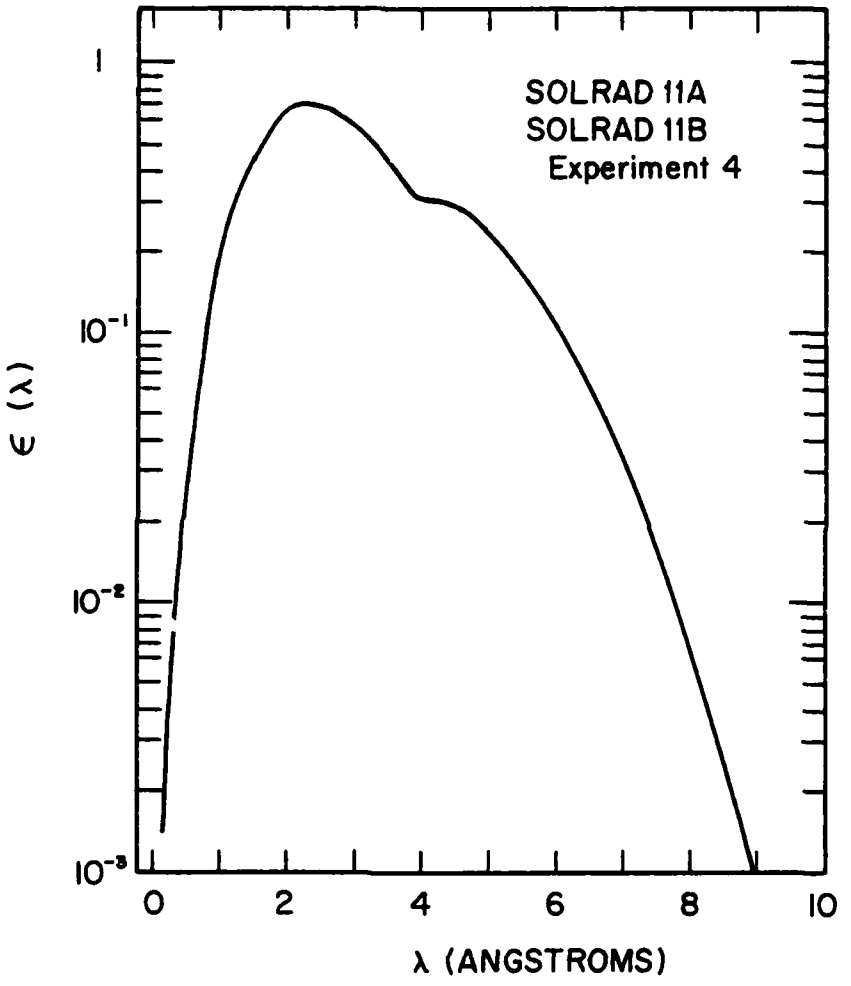

Fig. 6 — Efficiency of the 1 to 8 Åsensors of experiment 4 as a function of x-ray wavelength

voltage from the electrometer-amplifier in response to the input current generated by the ionization chamber. In the case of the linear electrometer-amplifiers the telemetered output voltage in digital counts is related to the detector current by

$$D = m_i I + b_i \qquad (4)$$

where m_i and b_i are the slope and intercept, respectively, for range i. Therefore the conversion from telemetered digital voltage levels to solar energy flux is accomplished by

$$F = \frac{K}{A\, m_i}(D-b_i) \qquad (5)$$

and values for m_i and b_i are given below.

Satellite	Detector	Range	m_i (counts/amp)	b_i (counts)
11A	4A	1	2.365(15)	12
		2	1.023(14)	11
		3	5.023(12)	10
		4	2.243(11)	10
	4B	1	2.166(15)	20
		2	1.069(14)	11
		3	5.241(12)	6
		4	2.363(11)	10
11B	4A	1	2.202(15)	16
		2	1.069(14)	9
		3	5.040(12)	6
		4	2.302(11)	10
	4B	1	2.287(15)	-2
		2	1.048(14)	9
		3	5.157(12)	6
		4	2.318(11)	10

Table 2 provides factors to convert fluxes for SOLRAD 9 and SOLRAD 10 to the new K values based on the efficiency measurements. Therefore, to compare SOLRAD 11 x-ray data with that from SOLRAD 9 or SOLRAD 10, the older satellite's graybody flux values should be multiplied by the indicated factor.

Table 2

Factors to convert SOLRAD 9 and SOLRAD 10 data to measured efficiency basis for comparison with SOLRAD 11 data.

Satellite	Band (Å)	Experiment No.	Conversion Factor
SOLRAD 9	0.5-3	7B	1.22
	1-8	6A	2.12
	1-8	6B	2.08
	8-20	5A	1.58
	8-20	5B	1.50
SOLRAD 10	0.5-3	1A	1.54
	0.5-3	1B	1.71
	1-8	3A	2.25
	1-8	3B	2.56
	8-20	4B	1.10

Experiment 5, 8 to 16 Å Ionization Chamber:

Experimenters: R.W. Kreplin, D.M. Horan, K.P. Dere, R.G. Taylor, Code 4170, Naval Research Laboratory

This experiment uses ionization chambers to measure solar emission over the 8 to 16 Å x-ray band. Similar sensors have been carried on all SOLRAD series satellites since SOLRAD 3 in 1961, thus providing 8 to 16 Å measurements over one eleven year solar cycle. The percentage changes in the 8 to 16 Å emission, either over a solar cycle or during solar flares, are smaller than 1 to 8 Å flux changes. The 8 to 16 Å flux is less significant geophysically than the 1 to 8 Å flux in that

its known effects are overshadowed by those caused by the 1 to 8 Å flux changes. Measurements of 8 to 16 Å flux during solar flares can be analyzed with measurements from experiments 4, 12, and 13 to calculate a differential emission measure versus temperature curve for the flaring plasma (Dere, et al., 1974) and thus provide a reasonably accurate solar emission spectrum over the 1 to 20 Å band.

Experiment 5 is identical to experiment 4 except that ionization chambers sensitive to 8 to 16 Å x-rays are used and the time interval between samples is different. The time interval for experiment 5 is 15.0 seconds in format 1, 30.0 seconds in format 2, and 7.5 seconds in formats 3 and 4. Table 1 gives pertinent information for the 8 to 16 Å sensors and values for K, A, ω, and ρx obtained, as for the 1 to 8 Å sensors, by fitting a curve to measured efficiency values. Figure 7 gives the fitted curve for the detector efficiency. Although the ionization chamber is virtually insensitive to wavelengths longer than 16 Å, K is calculated for the 8 to 20 Å band based on the assumed graybody spectrum at 2×10^6 K. Values for m_i and b_i (Eq. 5) are given below.

Satellite	Detector	Range	m_i (counts/amp)	b_i (counts)
11A	5A	1	2.325(15)	16
		2	1.022(14)	11
		3	5.136(12)	10
		4	2.298(11)	10
	5B	1	2.163(15)	-1
		2	1.042(14)	10
		3	5.176(12)	10
		4	2.262(11)	10
11B	5A	1	2.405(15)	-9
		2	1.030(14)	11
		3	5.152(12)	5
		4	2.296(11)	10
	5B	1	2.331(15)	10
		2	1.040(14)	10
		3	5.123(12)	10
		4	2.296(11)	10

Table 2 provides factors to convert fluxes for SOLRAD 9 and SOLRAD 10 to the new K values based on the efficiency measurements. Therefore, to compare SOLRAD 11 x-ray data with that from SOLRAD 9 or SOLRAD 10, the older satellite's graybody flux values should be multiplied by the indicated factors. It is interesting to note that when the SOLRAD 9 and SOLRAD 10 fluxes are both converted

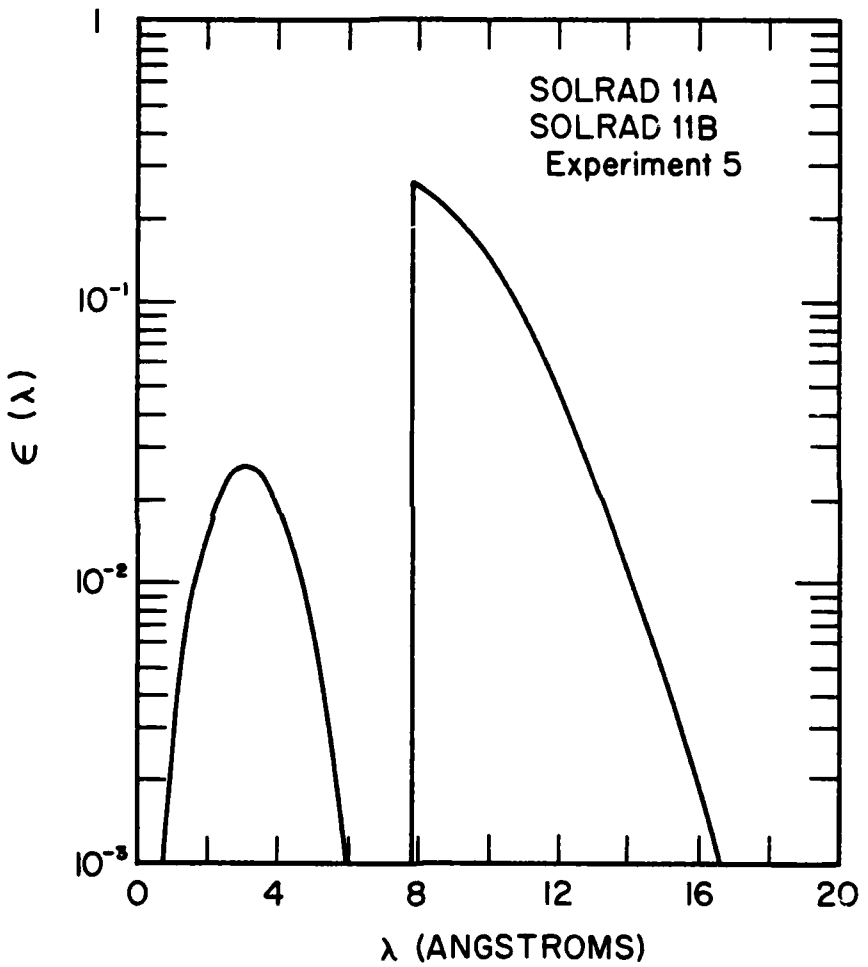

Fig. 7 — Efficiency of the 8 to 16 Åsensors of experiment 5 as a function of x-ray wavelength

using the factors in Table 2, a previously unresolved discrepancy between the two satellites' 8 to 20 Å flux levels (Horan and Kreplin, 1972) is resolved.

Experiment 6, 44 to 60 Å Ionization Chamber:

Experimenters: R.W. Kreplin, D.M. Horan, K.P. Dere, R.G. Taylor, Code 4170, Naval Research Laboratory

This experiment uses an ionization chamber to measure solar emission over the 44 to 60 Å band. Similar sensors have been carried on all SOLRAD series satellites since SOLRAD 7A in 1964. However, the sensors on satellites prior to SOLRAD 11 rarely had a lifetime longer than a few months so an extensive data base for this band is not available. The earlier failures seemed to be due to gas leakage through the Mylar window because of permeability or small holes developing. The earlier sensors had a Mylar window of approximately 1 inch diameter shielded by a metal plate to reduce the aperture. The sensor used on SOLRAD 11 has a metal window with a Mylar covered opening about 0.25 inch in diameter.

The experiment consists of an ionization chamber and a four-range electrometer-amplifer. The 0 to 5 volt analog output from the amplifier represents an instantaneous measurement of the current generated in the ionization chamber. It is converted to an 8 bit digital level and telemetered within a few milliseconds of taking the sample. The time interval between samples is 30 seconds in formats 1, 2, and 4 and 120 seconds in format 3. The range changing and amplifier calibration occur exactly as described for experiment 4. However, experiment 6 has the additional capability to calibrate the ionization chamber by moving a Am 241 source over the Mylar covered aperture on command. The source will remain in place over the aperture until commanded to move back to its stowed position. The indicator to show that the source was over the window failed on both satellites so the position of the source must be inferred from the ionization chamber data and command logs.

Table 1 gives pertinent information for the 44 to 60 Å sensors and values for K, A, ω and ρx obtained, as for the 1 to 8 Å sensors, by fitting a curve to measured efficiency values. A graybody solar spectrum for 0.5×10^6 K is assumed. Figure 8 gives the fitted curve for the detector efficiency. Values for m_i and b_i (Eq. 5) are given below.

Satellite	Range	m_i (counts/amp)	b_i (counts)
11A	1	2.223(15)	13
	2	1.012(14)	11

	3	5.139(12)	11
	4	2.322(11)	10
11B	1	2.291(15)	26
	2	1.027(14)	11
	3	5.033(12)	12
	4	2.289(11)	10

Although the ionization chamber used is quite sensitive to wavelengths shorter than 20 Å, Figure 8, the value of K is obtained with the assumption that all of the current generated in the chamber is due to 44 to 60 Å flux. The 44 to 60 Å flux levels obtained are estimated to be too large by about a factor of two when the Sun is quiet and by about an order of magnitude when the Sun is flaring. Recent SOLRAD satellites have carried an experiment sensitive to 1 to 20 Å emission which could be used to correct the 44 to 60 Å sensor's response to the 1 to 20 Å flux (Horan and Kreplin, 1972) but SOLRAD 11 does not carry a 1 to 20 Å sensor.

Experiment 7, 100 to 1030 Å - Three Bands:

Experimenters: R.W. Kreplin, D.M. Horan, R.G. Taylor,
Code 4170, Naval Research Laboratory

This experiment uses three LiF photosensitive surface detectors shielded by appropriate filters to monitor three subbands within the 100 to 1030 Å extreme ultraviolet (EUV) band which is important in the formation and variation of the ionospheric E and F layers. SOLRAD 10 was the first SOLRAD series satellite to attempt long-term measurements in the EUV band (Horan and Kreplin, 1972). Within a few months after launch in 1971 the signal decayed into the noise level. A four-range electrometer-amplifier is used with each of the detectors on SOLRAD 11. The sensitivity decrease experienced by each of the sensors during the first four months in space stabilized well above the noise levels of the amplifiers. Detector 7A is shielded by beryllium filters which limit its sensitivity to the 100 to 500 Å range. Detector 7B uses tin filters and is sensitive to 500 to 800 Å radiation. Detector 7C has indium filters which pass 700 to 1030 Å radiation. Two filters of the same material are attached in front of each detector so that small holes developing in a filter will probably not result in full spectrum sunlight striking the photosensitive surface. There is no redundancy in this experiment because the three different filter materials used permit measurements in different regions of the EUV spectrum.

The 0 to 5 volt analog output of each amplifier, which represents an instantaneous current measurement, is immediately subjected to 12 bit A-D conversion and telemetered within a

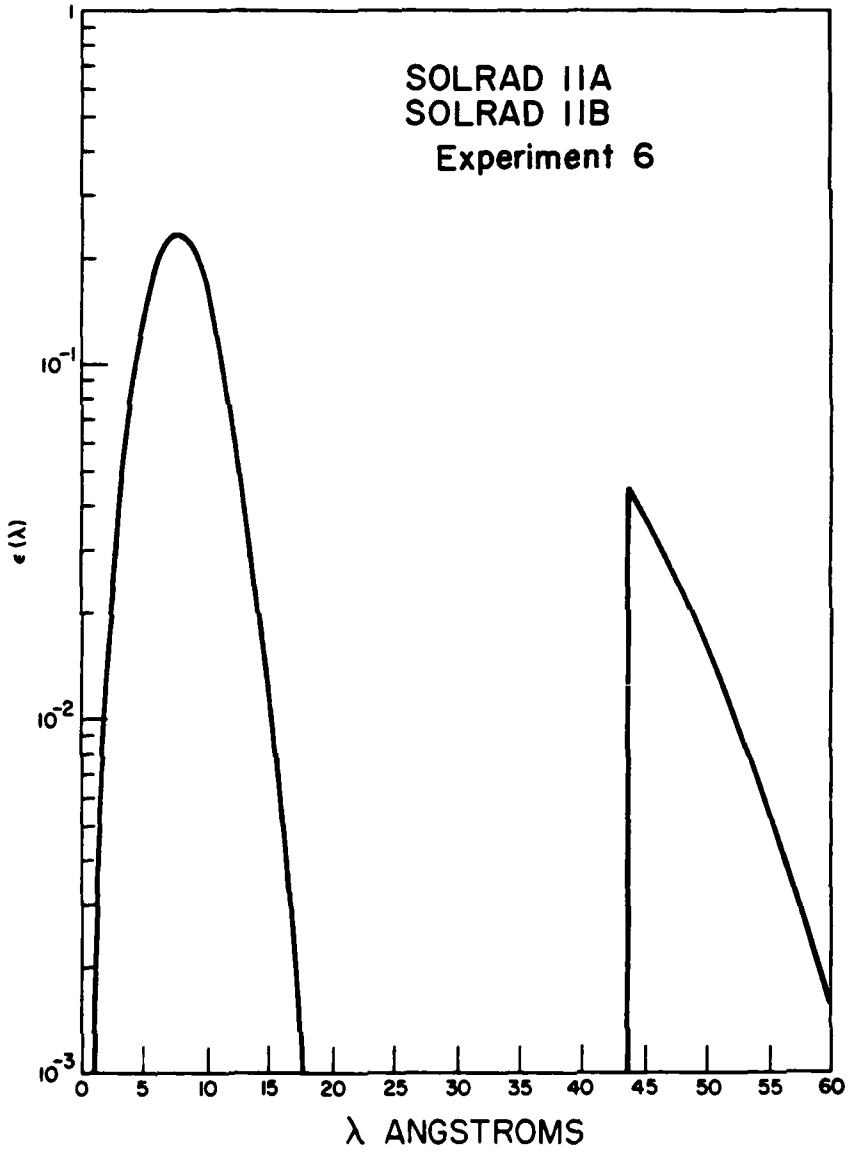

Fig. 8 — Efficiency of the 44 to 60 Åsensors of experiment 6 as a function of x-ray wavelength

few milliseconds after sampling. Each of the three amplifiers is sampled at 7.5 second intervals in formats 1 and 2. Experiment 7C only is sampled at 7.5 second intervals in format 4. Since all 12 bits of a telemetry word are needed to carry the amplifier's output voltage, the amplifer's range identification is not made when the output voltage is sampled. In the case of the amplifiers for 7B and 7C, the range is identified 3.75 seconds after the amplifier's output voltage is sampled. This situation requires a bit of caution in interpreting the telemetry. Fortunately the EUV flux is so stable that range changes are usually rare and multiple range changes within a few seconds are impossible. The amplifier range for 7A is identified and telemetered about 0.25 seconds after the amplifier output and range changes during that short interval should be extremely rare. Range changing and amplifier calibration occur exactly as described for experiment 4. Each of the amplifiers for experiment 7 is completely independent for range changing. Table 3 gives pertinent information for the detectors and filters used in experiment 7.

Table 3

EUV and UV Sensor Values

Experiment		7A	7B	7C	8A	8B
Band (Å)		100-500	500-800	700-1030	1120-1350	1120-1400
Filter/Window		1000Å Be	1600Å Sn	1700Å In	MgF_2	MgF_2
Cathode		LiF	LiF	LiF	—	NaCl
Gas: Pressure		—	—	—	NO:20mm	—
Area (cm^2)	11A:	0.71	0.71	0.71	1.6(-4)	7.9(-4)
	11B:	0.71	0.71	0.71	1.6(-4)	8.6(-4)
K $\left(\frac{erg}{sec\ amp}\right)$	11A:	5.42(10)	6.65(10)	3.32(11)	2.05(8)	2.43(9)
	11B:	1.28(11)	4.79(10)	2.88(11)	2.10(8)	2.87(9)
K' $\left(\frac{photons}{sec\ amp}\right)$	11A:	7.17(20)	2.16(21)	1.31(22)	1.27(19)	1.49(20)
	11B:	6.75(20)	1.53(21)	1.68(22)	1.28(19)	1.75(20)

Key: $7.32(20) = 7.32 \times 10^{20}$

The current generated by the photosensitive surface detectors can be expressed as

$$I = eA\int_0^\infty \tau_1(\lambda)\,\tau_2(\lambda)\,Y(\lambda)\,N(\lambda)\,d\lambda \qquad (6)$$

where e is the electronic charge, A is the aperture area, τ_i is the transmittance of the ith filter, Y is the photoelectric yield of the surface as ejected electrons per incident photon, and N is the solar emission spectrum as photons/cm^{2}sec Å. The transmittance of each filter of a pair of filters was measured individually using radiation at discrete wavelengths. A curve $\tau(\lambda)$ versus λ approximating the shape of those given by Samson (1967) for the appropriate filter material was then drawn through the measured transmittance values. The photoelectric yield at discrete wavelengths of each LiF photosensitive surface was then measured relative to a reference detector calibrated by the National Bureau of Standards. A curve $Y(\lambda)$ versus λ approximating in shape that given by Samson for LiF photoelectric yield was drawn through the measured values. Then the efficiency $\mathcal{E}(\lambda)$ of the detector-filter combination was found from the product

$$\mathcal{E}(\lambda) = \tau_1(\lambda)\,\tau_2(\lambda)\,Y(\lambda) \qquad (7)$$

and $\mathcal{E}(\lambda)$ versus λ is shown for the three detectors in Figure 9. The constant K required to convert from current generated in the detector to incident EUV energy flux

$$K = \frac{\int_{\lambda_a}^{\lambda_b} N(\lambda)\,hc\lambda^{-1}\,d\lambda}{e\int_0^\infty \mathcal{E}(\lambda)\,N(\lambda)\,d\lambda} \qquad (8)$$

was calculated using the spectrum of Donnelly and Pope (1973). A constant K' to convert from generated current to EUV photon flux

$$K' = \frac{\int_{\lambda_a}^{\lambda_b} N(\lambda)\,d\lambda}{e\int_0^\infty \mathcal{E}(\lambda)\,N(\lambda)\,d\lambda} \qquad (9)$$

was calculated also. As for experiment 4 the flux in a wavelength band λ_a to λ_b striking the top filter is obtained from the telemetered values by

$$F(\lambda_a, \lambda_b) = \frac{K}{A\,m_i}(D - b_i) \qquad (10)$$

where the flux is in ergs/cm^2 sec for K or photons/cm^2 sec for K', m_i and b_i are the slope and intercept for amplifier range i,

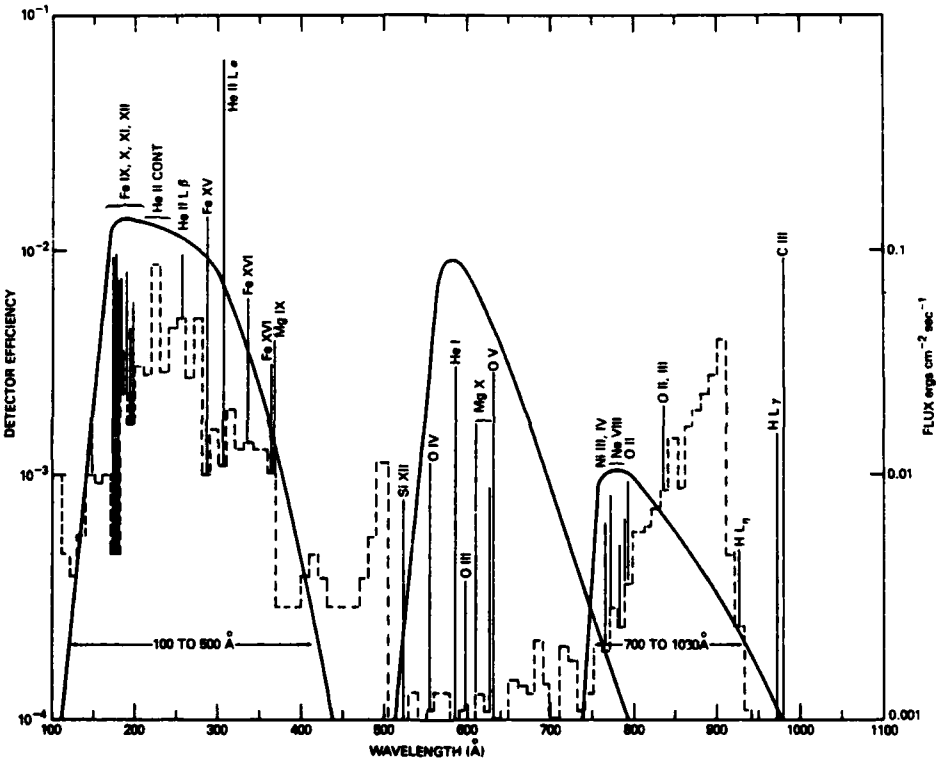

Fig. 9 — Efficiency of EUV sensors of experiment 7 as a function of wavelength and superposed on the EUV spectrum of Donnelly and Pope (1973)

A is the aperture area, and D is the telemetered output voltage in digital counts. Values for K and K' are given in Table 3. All values given are based on pre-launch measurements of the filter transmittances and photoelectric yields. Values for m_i and b_i follow.

Satellite	Detector	Range	m_i (counts/amp)	b_i (counts)
11A	7A	1	3.858(16)	-19
		2	1.709(15)	156
		3	8.749(13)	118
		4	3.897(12)	166
	7B	1	3.857(16)	71
		2	1.690(15)	163
		3	8.540(13)	109
		4	3.857(12)	162
	7C	1	3.795(16)	-90
		2	1.746(15)	156
		3	8.489(13)	130
		4	3.837(12)	163
11B	7A	1	3.864(16)	148
		2	1.769(15)	166
		3	8.606(13)	120
		4	3.893(12)	163
	7B	1	3.932(16)	-98
		2	1.798(15)	165
		3	8.666(13)	77
		4	3.887(12)	160
	7C	1	3.882(16)	178
		2	1.729(15)	165
		3	8.540(13)	139
		4	3.891(12)	166

During the first few months of flight changes occurred which significantly reduced the overall efficiencies for 7A, 7B, and 7C. However, corrections for the sensitivity decrease have not yet been calculated. One effect of the sensitivity change was a decrease in the current produced in the 7B detector on SOLRAD 11B by the most frequently encountered solar condition, i.e. nonflaring, to the point where the current fell between range 2 and range 3 of the electrometer-amplifier. This caused a constant cycling of the amplifier between the two ranges until it was commanded to manual range change mode and locked in range 3.

Transient currents generated in the amplifier during the range changes contaminated at least half of the telemetered values for Experiment 7B and interpretation of the remainder is not routine because the range identification is not simultaneous with the current measurement.

Experiment 8, 1080 to 1350 Å Ionization Chamber:

Experimenters: R.W. Kreplin, D.M. Horan, R.G. Taylor,
Code 4170, Naval Research Laboratory

This experiment uses two ionization chambers and a NaCl photosensitive surface detector to monitor solar ultraviolet radiation in the 1120 to 1400 Å band which is overwhelmingly dominated by the Lyman-α line of hydrogen at 1216 Å. Ionization chambers sensitive to this band have been carried on all SOLRAD series satellites starting with SOLRAD 1 in 1960. However, an extensive, continuous data base does not exist for this ultraviolet band, largely due to short-lived satellites in the 1960's and short-lived sensors in the 1970's. The best success in monitoring this band occurred from late 1965 to 1970 with sensors aboard SOLRAD 8 and SOLRAD 9. However the data is quite limited because the satellites were in a low Earth orbit and lacked data storage capability, which resulted in daily data accumulations only during 2 to 10 passes of about 10 minutes duration each over the ground station. In addition, the data processing techniques used with SOLRAD 8 did not result in a data library which is easily accessible, and the improved techniques used with SOLRAD 9 focussed on the X-ray data from the spacecraft's memory rather than the real-time telemetry which contained the UV data. The UV data from SOLRAD 10, launched in July 1971, was recorded in the satellite's memory and processed for easy retrieval, but the detector's sensitivity decreased rapidly after launch and within 7 months the output signal dropped to the noise level of the amplifiers. Although the same type sensor was used on SOLRAD 10 as had been carried on SOLRAD 8 and SOLRAD 9, a change in the roll axis orientation for SOLRAD 10 caused its sensor to be exposed to about four times as much solar radiation per unit time. Since SOLRAD 11 has the same roll axis orientation as SOLRAD 10, changes in the sensor were necessary to avoid rapid sensitivity loss. Therefore, MgF_2 windows were substituted for the LiF windows used in the ionization chambers on SOLRAD 9 and SOLRAD 10. A MgF_2 filter was placed in front of the NaCl photosensitive surface. The two ionization chambers on SOLRAD 11 are shielded from the Sun's rays by a movable shutter and the photosensitive surface detector is constantly exposed to the Sun. Thus the photosensitive surface detector performs the constant monitoring task and the shutter in front of the ionization chambers is periodically commanded open to calibrate the response of the NaCl surface detector. This

approach was not completely successful. The ionization chambers on SOLRAD 11A failed to operate after launch. The ionization chambers on SOLRAD 11B were used to calibrate the NaCl sensors on both satellites but the NaCl detectors' output signals both decayed into the noise level within a few months. Then the shutter in front of the ionization chambers was opened for extended periods so they could perform the monitoring task, but the shutter stuck in the closed position in early 1977.

The two ionization chambers are connected in parallel and designated 8A. The photosensitive surface detector is designated 8B. Either 8A or 8B can be connected to the experiment's single four-range electrometer-amplifier by command. The 0 to 5 volt analog output from the amplifier, representing an instantaneous measurement of the current generated in the sensor, is subjected to 12-bit A-D conversion and telemetered within a few milliseconds of taking the sample. The time interval between samples is 15 seconds. Since all 12 bits of a telemetry word are needed to carry the amplifier's output voltage measurement, the amplifier's range identification is not made when the output voltage is sampled. The range identification is made and telemetered at 7.5 second intervals which fall 3.25 seconds before and 4.25 seconds after the telemetry word carrying the output voltage measurement. This situation requires some caution in interpreting the telemetry but the solar Lyman-α flux is so stable that range changes are very rare. Range changing and amplifier calibration occur exactly as described for experiment 4. Table 3 gives pertinent information for the sensors used in experiment 8.

Although the experiment 8 detectors are sensitive to UV radiation over the band from about 1100 to 1400 Å, this band is so strongly dominated by the hydrogen Lyman-α line at 1216 Å that the current generated in the ionization chambers, given by Eq. 2 , can be approximated by

$$I = e \omega A \epsilon(\lambda) E(\lambda) \Delta\lambda \Big|_{1216} \qquad (11)$$

or for the photosensitive surface detector of 8B

$$I = e A \tau(\lambda) Y(\lambda) N(\lambda) \Delta\lambda \Big|_{1216} \qquad (12)$$

Following Eq. 3 the constant K required to convert from detector current to incident Lyman-α energy flux is given by

$$K = \frac{1}{e \omega \epsilon(\lambda)} \Big|_{1216} \qquad (13)$$

for the experiment 8A ionization chambers or following Eq. 8

$$K = \frac{hc\ \lambda^{-1}}{e\tau(\lambda)\ Y\ (\lambda)} \Bigg|_{1216} \qquad (14)$$

for the photosensitive surface detector, 8B. The conversion to photon flux is given by

$$K' = \frac{\lambda}{hce\omega\varepsilon(\lambda)} \Bigg|_{1216} \qquad (15)$$

for the ionization chambers or

$$K' = \frac{1}{e\tau(\lambda)\ Y\ (\lambda)} \Bigg|_{1216} \qquad (16)$$

for the photosensitive surface detector. Measurements of each detector's response to a Lyman-α beam were made and compared to a calibrated detector in order to determine $\omega\varepsilon(\lambda)$ for the ionization chambers and $\tau(\lambda)\ Y\ (\lambda)$ for the NaCl photosensitive surface detectors.

The Lyman-α flux incident on the detectors is obtained from the telemetered values as in Eq. 10. Values for A, K and K' are given in Table 3. The values for K and K' are based on pre-launch measurements on the detectors. During the first few months of flight changes occurred in the photosensitive surface detectors which reduced their sensitivity until the output voltage from the amplifier dropped to the noise level. Corrections have not yet been calculated for use during the period of decreasing sensitivity. A cursory look at the data from the ionization chamber, 8B, shows no obvious decrease in sensitivity prior to the shutter sticking in the closed position in early 1977. Values for m_i and b_i (Eq. 10) follow.

Satellite	Range	m_i (counts/amp)	b_i (counts)
11A	1	3.702(16)	108
	2	1.675(15)	175
	3	8.482(13)	149
	4	3.814(12)	168
11B	1	3.812(16)	314
	2	1.752(15)	180
	3	8.503(13)	163
	4	3.846(12)	167

Experiment 9, Ultraviolet Spectrometer:

Experimenter: P.D. Feldman, Code 4130, Naval Research Laboratory

This experiment uses a 1/8 meter Ebert-Fastie spectrometer to measure solar ultraviolet radiation between 1175 and 1800 Å in steps of 25 Å or 3.125 Å. Incident solar radiation passes through a curved slit in the focal plane of a spherical concave mirror and is reflected onto a reflection grating. The grating is rotatable to reflect the first order principal maximum of ultraviolet radiation over the 1175 to 1800 Å band back to the spherical mirror and thence to a curved exit slit in the mirror's focal plane. The optical system is basically as described by Fastie (1952). A photomultiplier tube is positioned behind the exit slit. The aluminum-coated, spherical, concave mirror has a 125 mm focal length. The grating is ruled with a density of 3600 lines/mm. Both mirror and grating are coated with MgF_2 to enhance reflectivity. The stepping motor which rotates the grating can be moved at two rates, selectable by command. At the faster scanning rate the entire 625 Å range is covered in 93.75 seconds. Each telemetered data word then contains data from a 25 Å band. The slower scanning rate covers the 625 Å range in 12.5 minutes and each telemetered data word pertains to a 3.125 Å band. The motion of the grating is controlled by a cam which allows uniform motion over the 1175 to 1800 Å range and then a rapid return of the grating to the starting position. The stepping motor is commandable into a high or low torque mode. The high voltage power supply can be commanded to 8 output levels. Counts in the photomultiplier are pre-scaled by a factor of 8 before reaching the FPA.

One 12-bit data word every 3.75 seconds is required to carry primary data. The content of each data word depends on the scanning rate. At the fast scanning rate a complete cycle is accomplished during, and in synchronization with, each TMTC. In the fast scanning mode the content of the 32 words used for primary data is as follows: the first word is a control word which provides unmistakable identification of the start of a scan and indicates the scanning rate, the high voltage setting, and the motor torque selected; the second through 26th words contain spectral data for 25 Å increments with the second word associated with the nominal 1175 to 1200 Å increment and the 26th word associated with the nominal 1775 to 1800 Å increment; the 27th and 28th words contain spectral data obtained while the grating is rapidly returning to its starting position (fly-back data); the 29th through 31st words contain dark count data which indicates the spurious count rate in the photomultiplier; and the last word contains the number of pulses used to step the motor during the full cycle of the cam. The control word which starts every scan, whether in fast or slow scan mode, always has the first five bits in the one state. The control word is unmistakable because it is never found anywhere except in the first frame of a telemetry cycle and its numerical content reflects a count rate

twelve times greater than the maximum expected count rate. If the last bit of the control word is in the one state, the instrument is executing a fast scan and the stepping motor pulse count will be found in the last frame of the TMTC. The stepping motor pulse count is telemetered from a 12 bit linear accumulator and the expected count is 3489. The telemetered count should be within $\pm$ 10 of the expected value to indicate proper operation of the instrument. Spectral data, fly-back data, and dark count data in the second through 31st frames is the telemetered output of an FPA which is incremented a single count for every eight counts generated by the photomultiplier.

In the slow scanning mode seven TMTC's, 224 frames of 3.75 seconds each, are required to telemeter the control word, spectral data, fly-back data, dark count data, and motor pulse count. The control word is the first word of the scan and is always found in the first frame of a TMTC. Slow scan is indicated when the last bit of the control word is in the zero state. The second through 201st words of the scan contain spectral data with the second word associated with a nominal 1175 to 1178.1 Å band and the 201st word associated with a nominal 1796.9 to 1800 Å band. The 202nd through 217th words contain fly-back data; the 218th through 223rd words contain dark count data; and the 224th and last word contains the motor pulse count. The expected motor pulse count is 3489, as for the fast scanning mode.

Spectrometer scans are synchronizd with the spacecraft's TMTC. When a scan is finished the instrument waits until the beginning of the next TMTC before beginning the next scan. At the beginning of the first 3.75 second frame of the telemetry cycle, the grating begins to rotate in discrete steps - about 128 per frame for the fast scan rate and about 16 per frame for the slow scan rate. Data accumulation time is 3.75 seconds and data accumulated during one frame is telemetered during the next frame. The grating continues to rotate until it returns to its starting position, where it waits for the next TMTC to begin. If a command to change the scanning rate is received during a scan, the relay which controls the scanning rate will immediately change, but the instrument will not change its grating rotation speed until the beginning of the next scan. Therefore, the relay position indicator is not absolutely reliable as an indicator of scanning rate. The control word at the beginning of each scan is the more reliable indicator.

The instruments were calibrated before launch by measuring their response to known intensities of ultraviolet radiation at discrete wavelengths. The conversion from experiment output to photon flux at specific wavlengths is given by

$$F_\lambda = K_\lambda \, C \ (\text{photons/cm}^2 \text{ sec Å}) \qquad (17)$$

where C is the telemetered counting rate. Table 4 gives the values of K_λ obtained from the laboratory calibrations of the flight

instruments. The pre-scaling by the instruments has been included in K_λ and therefore there is no need to multiply by 8 when using the value from Table 4 with the experiment output.

Table 4

Values of K_λ (10^6 photons/count cm^2 Å)

Wavelength (Å)	11A	11B
1177	----	2.19
1192	1.78	1.54
1216	1.14	0.904
1280	0.715	0.531
1336	0.653	0.496
1396	0.707	----
1463	0.827	0.629
1518	0.934	0.766
1545	1.10	0.899
1608	1.88	1.54
1639	2.02	1.69
1655	3.26	----
1670	----	2.33
1724	----	3.62
1731	5.71	----
1779	----	6.84
1793	18.2	----

Post-launch degradation in the photomultiplier tubes and optics caused a decrease in sensitivity. The ratio of measurements made in July 1976 to those made in March 1976 ranged from a value of 0.30 at the shorter wavelengths to 0.65 at the long wavelength end of the instruments' spectral range. Experience with the data from this experiment has shown that the data word immediately following a control word is incorrect. Data from the instrument on SOLRAD 11A frequently shows zero values or identical values in successive words. Zero values should never be encountered and repeated values should be extremely rare in valid data.

Experiment 10, Thomson X-ray Polarimeter:

Experimenter: G.A. Doschek, Code 4170, Naval Research Laboratory

This experiment is intended to detect polarized solar x-ray emission between 10 and 60 kev. Incident x-rays undergo Thomson scattering by a block of lithium. Scattered non-polarized x-rays are observed isotropically in a plane perpendicular to the direction

of incidence. Polarized x-rays are preferentially scattered in a direction perpendicular to the electric vector E. Two proportional counters are mounted so their windows are facing each other through the lithium block. As the satellite rolls, the block and detectors rotate with respect to the electric vector of incident polarized radiation. Electronic gating to separate data pulses associated with 45° sectors in the roll direction will reveal pulse count variations from sector to sector if polarized radiation is present in significant quantities. Since the Thomson scattering mechanism is symmetric about 180°, the eight roll direction sectors are paired with sectors one and five together, two and six, etc. The lithium block is sealed in beryllium to decrease sensitivity to lower energy x-rays. Two channel analysis is used to separate the output pulses from each detector into two energy groups - 10 to 22 kev (channel 1) and 22 to 60 kev (channel 2). Each of the two detectors has a set of eight FPA's (2 channels x 4 sectors) to register counts from scattered rays. Experiments 10 and 11 are mechanically aligned in the spacecraft so that they will be simultaneously responding to polarized solar radiation. The boundaries of their 45° sectors in the roll direction are electronically aligned. The spacecraft's roll reference system generates pulses at intervals of 1/8th of the roll period which gate the pulses from the detectors into different FPA's. The FPA's are read and reset to zero every thirty seconds starting at the beginning of each TMTC. After the FPA's are read and reset, they are prevented from accepting data until the first star pulse occurs as a reference in the roll orientation. Data is then accumulated for six complete spacecraft rolls and then the FPA's are locked until the next readout. Nominal roll period for the spacecraft is four seconds so there is a deadtime of approximately six seconds in every thirty second data cycle. Data accumulated during one thirty second period is telemetered during the next thirty second period.

Each detector contains two sets of electronic grids. Pulses generated by the set closest to the window are used as a measure of scattered x-rays. Simultaneous pulses from both sets of grids are accumulated separately as a measure of high energy charged particle interference, and labeled as coincidence counts. Pulses generated on the grids farthest from the windows are also accumulated separately and labeled background counts. The background and coincidence counts of each detector, accumulated for a full thirty seconds without gating by spacecraft sectoring or star pulses, are telemetered once during each TMTC. The thirty second accumulation periods coincide with those used for the data from Thomson scattering. Data accumulated during one thirty second period is telemetered during the next thirty second period.

In-flight adjustment of the energy channel bounds is achieved by use of Cd 109 as a source of 22 kev radiation and high voltage power supplies commandable to 16 output levels. When the calibration sequence is commanded, the radioactive source swings

between the detectors at the beginning of the next TMTC, remains there for the entire cycle, and then swings back into its shielded enclosure. The calibration sequence can be terminated before the end of two minutes by use of a separate command. Calibration of the detectors is accomplished by adjusting the high voltages until each detector's response to the radioactive source is equal in both channels.

Experiment 11, Bragg X-ray Polarimeter:

Experimenter: J.F. Meekins, Code 4120, Naval Research Laboratory

This experiment is designed to detect polarized solar x-ray emission near 2.8 Å. A LiF crystal is fixed at an angle of 45° to allow x-rays of approximately 2.8 Å to undergo first order Bragg reflection into a proportional counter. Reflection of polarized electromagnetic radiation is a function of the angle between the electric vector E and the plane of incidence. Rotation of the reflecting crystal as the satellite rolls will effectively change this angle. Electronic gating to separate data pulses associated with 45° sectors in the roll direction will cause signal variations from sector to sector if polarized radiation is present in significant quantities. Eight FPA's are used to register counts from the reflected x-rays. Experiments 10 and 11 are mechanically aligned in the spacecraft so that they will be simultaneously responding to polarized solar radiation. The boundaries of their 45° sectors in the roll directions are electronically aligned.

The spacecraft's roll reference system generates pulses at intervals of 1/8th of the roll period which gate the pulses from the detector into different FPA's. The FPA's are read and reset to zero at the start of each TMTC, and then prevented from accepting data until a star pulse occurs to provide a reference in the roll direction. Counts from reflected x-rays are then accumulated for 27 complete spacecraft rolls and the FPA's are then locked until the next readout. Nominal roll period for the spacecraft is 4 seconds so there is a deadtime of approximately 12 seconds in every two minute data acquisition cycle. Data accumulated during one TMTC is telemetered during the next cycle.

There is no capability for in-flight calibration of this instrument. However, the high voltage power supply is commandable to 16 output levels. For proper operation of this experiment it is necessary that the angle between the spacecraft's spin axis and the satellite-Sun line be less than 0.7°.

Experiment 12, 0.5 to 3 Å Ionization Chamber:

Experimenters: R.W. Kreplin, D.M. Horan, K.P. Dere, R.G. Taylor, Code 4170, Naval Research Laboratory

This experiment uses ionization chambers to measure solar emission in the 0.5 to 3 Å x-ray band. All SOLRAD series satellites since SOLRAD 8 in 1965 have carried ionization chambers or Geiger-Muller tubes to monitor this band. However, 0.5 to 3 Å x-ray emission above the sensitivity threshold of the experiment is only encountered during solar flares or when several active regions coexist on the visible disk. Therefore, there is no continuous record of 0.5 to 3 Å emission covering several years. The 0.5 to 3 Å measurements during solar flares can be analyzed with measurements from experiments 4, 5, and 13 to calculate a temperature and emission measure profile of the flaring plasma (Dere, et al., 1974) and to provide a reasonably accurate solar emission spectrum over the 1 to 20 Å band.

The experiment consists of three ionization chambers electronically connected in parallel to a four-range electrometer-amplifier. The three ionization chambers provide a large window area which increases sensitivity to the weak 0.5 to 3 Å emission when flares and active regions are absent from the visible disk. The 0 to 5 volt analog output from the amplifier represents an instantaneous measurement of the currents generated in the three ionization chambers. It is converted to an 8 bit digital level and telemetered within a few milliseconds of taking the sample. The time interval between samples is 7.5 seconds in formats 1, 3, and 4 and 15.0 seconds in format 2. The range changing and amplifier calibration occur exactly as described for experiment 4.

Table 1 gives pertinent information for the 0.5 to 3 Å sensors and values for K, A, ω, and ρx obtained, as described for the experiment 4 sensors, by fitting a curve to measured efficiency values. Figure 10 gives the fitted curve for the detector efficiency. Values for K are based on the measured efficiencies. A graybody solar spectrum for 1×10^7 K is assumed (Kreplin, 1961). Values for m_i and b_i (Eq. 5) follow.

Satellite	Range	m_i (counts/amp)	b_i (counts)
11A	1	2.224(15)	6
	2	1.069(14)	10
	3	5.203(12)	8
	4	2.358(11)	10
11B	1	2.281(15)	23
	2	1.038(14)	11
	3	5.184(12)	10
	4	2.306(11)	10

Table 2 provides factors to change SOLRAD 9 and SOLRAD 10 data to values based on the K values obtained from the measured efficiency. Therefore, data from older satellites should be multiplied by the indicated factors for comparison with SOLRAD 11.

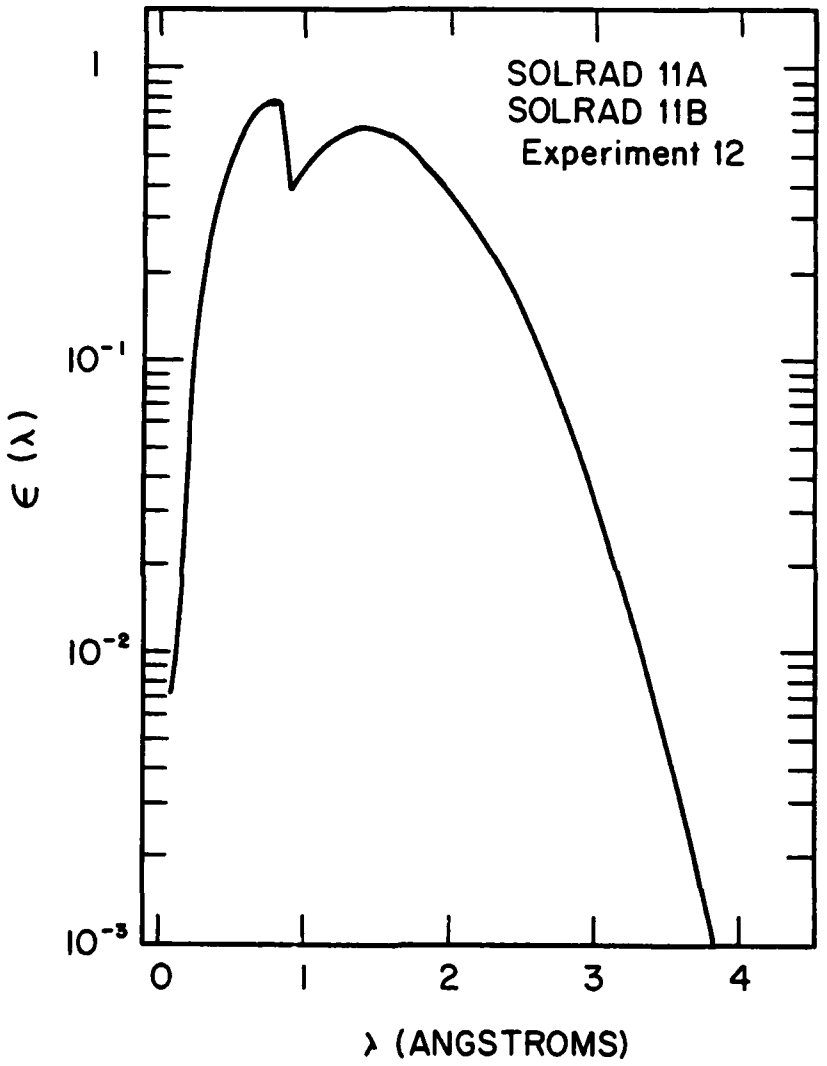

Fig. 10 — Efficiency of the 0.5 to 3 Åsensors of experiment 12 as a function of x-ray wavelength

Experiment 13, 2 to 10 Å Ionization Chamber:

Experimenters: R.W. Kreplin, D.M. Horan, K.P. Dere, R.G. Taylor, Code 4170, Naval Research Laboratory

SOLRAD 11 is the first SOLRAD series satellite to monitor the 2 to 10 Å band. An ionization chamber sensitive to 2 to 10 Å radiation is included on SOLRAD 11 to improve calculations of the emission measure versus temperature profile for the emitting coronal plasma. Measurements of the 2 to 10 Å flux can be analyzed with data from experiments 4, 5, and 12 to obtain the differential emission measure versus temperature curve and thus provide a reasonably accurate solar emission spectrum over the 1 to 20 Å band.

The experiment consists of an ionization chamber and a four-range electrometer-amplifier. The 0 to 5 volt analog output from the amplifier represents an instantaneous measurement of the current generated in the ionization chamber. It is subjected to 8 bit A-D conversion and telemetered within a few milliseconds of taking the sample. The time interval between samples is 15 seconds in format 1, 30 seconds in format 2, and 7.5 seconds in formats 3 and 4. The range changing and amplifier calibration occur exactly as described for experiment 4.

Table 1 gives pertinent details for the 2 to 10 Å sensors and values for K, A, ω, and ρx obtained, as for the 1 to 8 Å sensor, by fitting a curve to measured efficiency values. A graybody solar emission spectrum for 2×10^6 K is assumed (Kreplin, 1961). Figure 11 gives the fitted curve for the detector efficiency. Values for m_i and b_i (Eq. 5) follow.

Satellite	Range	m_i (counts/amp)	b_i (counts)
11A	1	2.404(15)	12
	2	1.080(14)	11
	3	5.115(12)	11
	4	2.334(11)	11
11B	1	2.279(15)	-4
	2	1.040(14)	10
	3	5.222(12)	6
	4	2.365(11)	10

Experiment 14, Solar Protons > 10 Mev:

Experimenter: J.B. Blake, The Aerospace Corporation, Los Angeles, California 90045

This experiment is intended to detect protons and alpha particles coming from the general direction of the Sun. The

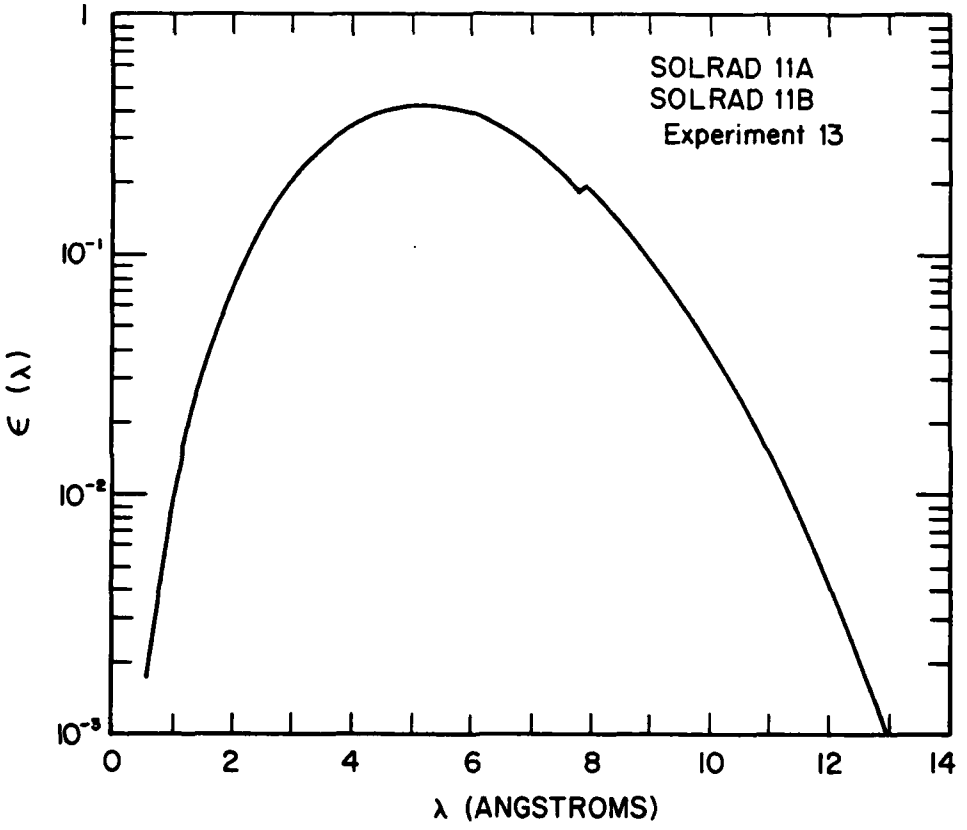

Fig. 11 — Efficiency of the 2 to 10 Åsensors of experiment 13 as a function of x-ray wavelength

instrument is a two element counter telescope using disk shaped semiconductors as detector elements with shielding material in front of and between the two detector elements. Penetration of the first shield provides a 2 Mev threshold for protons. Penetration of both shields and the first detector provides a 10 Mev threshold. Coincidence and pulse height analysis is used to separate pulses produced by protons, alpha particles, and heavier nuclei.

Four FPA's and a four bit linear accumulator count pulses during a full TMTC. The FPA's count protons in two energy ranges, above 2 Mev and above 10 Mev; and alpha particles in two energy ranges, above 4.5 Mev and above 7.5 Mev. Heavy nuclei with energy at or above 3 Mev per nucleon are counted by the linear accumulator. Data obtained during one TMTC is telemetered during the next TMTC.

There is no provision for in-flight calibration of this instrument.

Experiment 15, Solar Wind:

Experimenters: A.J. Lazarus, J. Sullivan, MIT
Cambridge, Massachusetts 02139

This experiment is designed to monitor the number density, temperature, and bulk velocity of the positive ion component of the solar wind and the number density and temperature of the solar wind electrons. The positive ion measurements are made with a modulated grid Faraday cup whose collector plate is composed of three 120° sectors. A positive ion spectrum is generated by stepping through positive DC biases on a high voltage grid and modulating at each bias level with a square wave at 500 hertz to form 24 contiguous energy windows. The complete positive voltage range is approximately 240 to 4300 volts. A positive ion total flux measurement is made by causing the voltage to oscillate between 240 and 4300 volts at 500 hertz. The relative currents from the three sectors of the collector plate are used to calculate the solar wind flow direction. The electron measurements are made with a modulated grid Faraday cup with a single collector plate. The negative voltage range is 16 to 115 volts divided into four contiguous energy windows. The instrument has two sampling modes, normal mode and flux mode. In normal sampling mode the instrument will generate 33 data words during a sampling cycle in the following sequence: identifier word, 24 positive ion energy channel samples, 4 electron energy channel samples, a positive ion total flux sample, and one sample from each of the three sectors of the positive ion cup collector plate. The sequence of 33 samples in flux mode begins with the identifier word which is then followed by six groups, each with the sequence of an electron total flux sample, a positive ion total flux sample, and 1 sample from each of the three sectors of the positive ion

cup collector plate. The final two samples in a flux mode sampling cycle are an electron total flux sample followed by a positive ion total flux sample.

Linear 8-bit registers are used for the data samples and the identifier word. The identifier word is a counter which increments once each sampling cycle. The value in the identifier word ranges from a 0 to 191 for normal mode sampling, and 192 to 255 for flux mode sampling. In normal sampling mode the instrument automatically produces three sets of calibration data during a 192 sample cycle of the identifier word. These calibration data sets appear with identifier word 0, 64, and 128 and provide the calibration levels for the DC voltage windows, the AC modulation voltages and the current. When the instrument is sampling in flux mode the calibration data sets are suppressed; but one sampling cycle out of 64, that with the identifier word value 192, is in the format of normal sampling mode data.

A sampling cycle lasts approximately 6.8 seconds in either sampling mode. However, the instrument can be commanded to start a sampling cycle every two minutes, or every 11.25 seconds. The thirty-three 8-bit words generated during each sampling cycle are telemetered as twenty-two 12-bit words. The faster repetition rate requires most of the satellite's telemetry capacity and therefore its use is severely restricted.

In order to obtain the speed, temperature, and density of the positive ion component of the solar wind from the normal mode data, the following steps are necessary. The telemetered data values, D, for the positive ion spectrum are converted as

$$F_j = \frac{A\ B^{(255-Dj)}}{V_j\ W_j} \qquad (18)$$

where $A=6.94 \times 10^{-13}$, $B=1.0367$, V_j is the mean velocity for the jth energy window, W_j is the velocity width of the jth window, and j specifies each data word from a 33 word data sample. Letting j=1 be the identifier word, j will range from 2 to 25 for the positive ion spectrum. Values for V_j and W_j are given in Table 5. The spectral window providing the maximum value for F_j is identified and its j value is designated as m. If m is not within the range $4 < m < 23$, calculations cease and another 33 word data sample is selected. If calculations are continued, three sums are formed as follows

$$S_o = \Sigma F_j\ W_j$$

$$S_1 = \Sigma V_j\ F_j\ W_j$$

$$S_2 = \Sigma V_j^2\ F_j\ W_j$$

over the range $m-4<j<m+4$. The desired positive ion parameters are then obtained from

$$\text{Speed} = S_1/S_o \quad \text{(km/sec)}$$

$$\text{Temperature} = 125.0\ [S_2/S_o) - (S_1/S_o)^2] \quad \text{(K)}$$

$$\text{Density} = 2.5\times10^{12}\ S_o \quad \text{(positive ions/cm}^3\text{)}$$

Additional information on this experiment can be found in "Analysis of Solar Wind Data From the SOLRAD 11A and 11B Spacecraft" by Alan J. Lazarus, AFGL-TR-79-0056, February 1979.

Table 5

Values of average velocity and velocity width of energy channels.

j	V_j	W_j
2	232.6	32.6
3	263.1	28.4
4	290.8	25.8
5	314.7	23.9
6	337.4	22.4
7	359.6	20.9
8	379.2	19.8
9	398.2	18.8
10	417.2	18.0
11	434.5	17.4
12	459.6	32.7
13	498.8	45.4
14	542.4	41.8
15	582.8	38.8
16	620.7	36.4
17	656.5	34.2

18	690.5	32.8
19	723.2	31.3
20	754.6	30.0
21	784.6	28.5
22	813.8	27.6
23	842.0	26.8
24	869.5	25.8
25	896.2	25.2

Experiment 16, Stellar/Auroral X-rays:

Experimenters: E.T. Byram, D.M. Horan, Code 4170, Naval Research Laboratory

The experiment is designed to map x-ray sources in the sky and to monitor auroral x-ray emission from the Earth. The detector is a large-windowed, 4 inches by 6 inches, proportional counter sensitive to 1 to 8 Å x-rays and mounted on the side of the satellite. On SOLRAD 11A the normal to the detector surface is perpendicular to the satellite's roll axis and parallel to the spacecraft radius passing through the detector. On SOLRAD 11B the detector's normal is co-planar with the local radius through the detector and the roll axis and tilted toward the Sun at a 35° angle to the local radius. As the satellite rolls, the detector sweeps a circular band which is divided into 64 sectors by the satellite's roll reference system. Eight 12 bit linear accumulators each accept data from one of the 64 sectors during a TMTC. Data acquired during one telemetry cycle is transmitted during the next cycle. Telemetered information identifies which eight of the sectors are the origins of data being telemetered. It takes eight telemetry cycles, sixteen minutes, to make stellar x-ray measurements completely around the roll plane. At the beginning of each TMTC the values in the linear accumulators are shifted into storage registers, the accumulators are set to zero, associated with a new set of sectors, and prevented from accepting pulses until the first star pulse occurs. Counts from the appropriate sectors of the roll plane are then accepted for 27 complete rolls of the spacecraft, and the accumulators are then locked for the remainder of the TMTC.

A ninth 12-bit linear accumulator accepts data from a single, movable sector equal to 1/32 of the circle swept by the detector. The location of this sector in the roll plane is controlled by Earth

pulses. The primary purpose of this movable sector is to point at the Earth when the Earth lies on the circle swept by the detector, but the sector can be pointed anywhere on the circle by means of commandable time delays for the Earth pulse. The first Earth pulse after the beginning of a telemetry cycle starts data acquisition for the movable sector, and the data acquisition continues for 27 complete rolls of the spacecraft. The accumulator is then locked for the remainder of the TMTC. Unless the movable sector is commanded to a different portion of the roll plane the same portion of the sky is observed during every telemetry cycle.

The detector used for this experiment is identical to those used for experiment 11, and background and coincidence counts from the double grids within the detector are measured and telemetered. Background data is telemetered during one telemetry cycle, and coincidence data on the next. A full two-minute acquisition time is used and counts are accumulated on an FPA.

Experiment 17, Omnidirectional Protons:

Experimenter: J.B. Blake, The Aerospace Corporation
Los Angeles, California 90045

This experiment uses seven sensors to measure particles of positive charge with energies ranging from 20 kev to 460 Mev. Five of the sensors, designated 17A1 through 17A5, are omnidirectional sensors. The other two sensors, 17C and 17D, have a more limited field of view. Each omnidirectional sensor comprises a small silicon cubic semiconductor centered under a hemispherical shield and heavily shielded relative to the hemispherical shield over the rear 2π solid angle. The five sensors differ in the thickness of the hemispherical shield and thus each has a different minimum energy level for electrons, protons, and alpha particles which penetrate to the silicon detector. Each detector is connected to a charge sensitive amplifier and a two level discriminator. In the energy range of interest the energy loss per unit path length, dE/dx, for protons is much greater than that for electrons, and less than that for alpha particles. The discriminator settings utilize this fact to reject electrons and distinguish between pulses caused by protons and alpha particles. The nominal energy ranges of particles counted by the omnidirectional sensors are given in Table 6. The omnidirectional sensors are mounted on the side of the spacecraft and use the roll motion of the spacecraft to collect data over a full 4π solid angle. A pair of FPA's are associated with each of the five omnidirectional sensors to count the protons and alpha particles detected during a full TMTC. Data obtained during one telemetry cycle is transmitted during the next cycle.

Table 6

Energy Ranges of Omnidirectional Sensors

Sensor	Protons (Mev)	Alpha Particles (Mev)
17A1	5-20	20-80
17A2	10-25	40-100
17A3	20-40	80-140
17A4	50-90	200-240
17A5	100-160	400-460

Sensors 17C and 17D are also mounted on the side of the spacecraft and use the satellite's roll motion to approach an omnidirectional capability. The field of view of each is a cone whose axis is parallel to a spacecraft radius. The field of view of 17C has a 30° half-angle and 17D has a 10° half-angle field of view. Sensor 17C consists of a photomultiplier tube viewing a thin plastic scintillation foil. Pulse height analysis is used to separate pulses from ions of varying charge. Sensor 17D uses a pair of disk shaped semiconductors as detector elements. The detectors are connected to charge sensitive amplifiers. Coincidence and pulse-height analysis are used to determine the proton flux in eight energy channels. The type of particles counted, the energy range, and the channel labels associated with sensors 17C and 17D are given in Table 7.

Table 7

Energy Ranges of Sensor 17C and 17D

Sensor	Channel	Particle	Range
17C	P14	Protons	E >0.5 Mev
	A12	Alpha Particles	E >0.5 Mev/nucleon
	H6	$6 \leq Z \leq 10$	E >0.6 Mev/nucleon
	H7	$12 \leq Z \leq 18$	E >0.7 Mev/nucleon

	H8	$Z \leq 18$	E >0.8 Mev/nucleon
17D	P10	Protons	E >0.5 Mev
	P11	Protons	E >1.0 Mev
	P12	Protons	E >1.5 Mev
	L1	Protons	$20 \leq E \leq 36$ kev
	L2	Protons	$36 \leq E \leq 74$ kev
	L3	Protons	$74 \leq E \leq 150$ kev
	L4	Protons	$150 \leq E \leq 280$ kev
	L5	Protons	$280 \leq E \leq 500$ kev

Except for A12 and H6 of 17C and P11 and L2 of 17D each channel has one FPA to count the charged particles detected during a full TMTC. Data accumulation for A12 and H6 of 17C and P11 and L2 of 17D is controlled by the spacecraft's roll reference system which generates pulses at intervals of 1/4 of the roll period. Data from each of the four channels is gated into FPA's associated with 90° sectors in the roll direction. The sixteen FPA's associated with these channels are read and reset to zero at the start of each TMTC, and then prevented from accepting data until a star pulse occurs to provide a reference in the roll direction. Particle counts are then accumulated in the FPA's for 27 complete spacecraft rolls and then the FPA's are locked until the next readout. Nominal roll period for the spacecraft is four seconds so there is a dead time of approximately twelve seconds for these sectored channels during each TMTC. In the case of every channel for sensors 17C and 17D, data accumulated during one TMTC is telemetered during the next cycle.

There is no capability for in-flight calibration for any of the component sensors of experiment 17.

Experiments 18 and 19, Geocoronal - Extraterrestrial EUV:

Experimenters: C.S. Weller, Jr., R.R. Meier, Code 4140, Naval Research Laboratory

These experiments use a pair of continuous channel photo-electron multipliers operating in a pulse count mode to measure EUV and UV radiation from non-solar sources. One detector is experiment 18 and the other is experiment 19 but they are controlled and operated as a single unit. A filter wheel can be rotated to

place different window materials between each detector and its collimator to permit isolation of specific emission lines in the wavelength range between 200 and 1400 Å. The detectors are mounted on the side of the spacecraft and look in a direction perpendicular to the satellite's roll axis and parallel to the radius through the mounting position. Open collimators limit the field-of-view to 9° full width at half maximum.

As the satellite rolls the detectors sweep a great circle which is divided into 64 sectors by the satellite's roll reference system. Eight FPA's are associated with each detector. Each FPA accepts data from one of the 64 sectors during each sampling roll of the spacecraft. Eight sampling rolls occur during each TMTC so all 64 sectors are observed every two minutes. At 15 second intervals synchronized with the beginning of the TMTC the values in the FPA's are shifted into storage registers for telemetering, the FPA's are reset to zero, associated with a new set of sectors, and prevented from accepting pulses until the next star pulse occurs. Data from eight sectors is then accumulated during one complete roll and then the FPA's are locked until the beginning of the next 15 second interval. Data obtained during a given 15 second interval is telemetered during the next 15 second interval. Since experiments 18 and 19 were not to be on continuously, data from these experiments is transmitted only when telemetry format 2 is used.

A ten-position wheel can be rotated in-flight to place different windows in front of the two detectors. An analog monitor indicates the position of the filter wheel. The correspondence between the analog monitor's voltage and the material in front of the detectors is given in the following table:

Analog	SOLRAD 11A		SOLRAD 11B	
Voltage	Exp 18	Exp 19	Exp 18	Exp 19
0.2	Open	Sn	Source	Open
0.7	MgF_2	Al	Blank	Open
1.3	Al - C	Al	CaF_2	MgF_2
1.9	Sn	Source	Open	Al - C
2.5	Al	Blank	Open	Sn
3.0	Al	CaF_2	MgF_2	Al
3.6	Source	Open	Al - C	Sn
4.1	Blank	Open	Sn	Source
4.7	CaF_2	MgF_2	Al	Blank
5.0	Open	Al - C	Sn	CaF_2

A blank space in the filter wheel indicates that incident radiation is prevented from reaching the detector. The Fe 55 radioactive source is used for calibration. The high voltage power supplies can be commanded to 16 output levels. Two high voltage power supplies are carried for redundancy.

Experiment 20, Proton-Alpha Telescope:

Experimenters: J.G. Kelley, L. Katz, G.K. Yates, Air Force Geophysical Laboratory, Bedford, Massachusetts, 01730

Two totally depleted silicon suface barrier detectors are used to detect 1 to 100 Mev protons and 10 to 100 Mev alpha particles. The telescope consists of a 200 micron front detector and a 750 micron rear detector separated by 2.26 cm. Each detector is 2 cm^2 in area. Pulse height analysis of dE/dx in each detector is used to measure the incident particle spectrum. The telescope accumulates data in three modes simultaneously - individual modes for each detector and a coincidence mode. In the coincidence mode eight sets of discriminator settings for the 200 and 750 micron detectors separate the incident protons into 5 energy ranges between 5 and 100 Mev and the incident alpha particles into three energy ranges between 22 and 100 Mev. In the coincidence mode the effective area of the detectors is reduced to 1.27 cm^2. Pulse height analysis of dE/dx in the 200 micron detector separates protons with energy between 1.24 and 6.6 Mev into 6 channels, and alphas with energy between 10.7 and 16.1 Mev into a single channel. Incident protons and alpha particles are separated into the following energy channels.

Protons (Mev)	Alphas (Mev)
1.24 - 1.35	10.7 - 16.1
1.35 - 1.56	22.0 - 32.0
1.56 - 2.01	32.0 - 52.0
2.01 - 2.69	52.0 - 100
2.69 - 4.03	
3.64 - 6.58	
5.50 - 8.00	
8.00 - 13.0	
13.0 - 25.0	
25.0 - 50.0	
50.0 - 100	

The telescope's aperture is covered by a thin aluminum foil to exclude light and low energy electrons. Higher energy electrons are effectively rejected by the dE/dx threshold settings. An Am 241 radiation source constantly stimulates the detectors. When solar particle flux is low the source signature can be used to verify the discriminator settings of the dE/dx windows. The source contribution is negligible in comparison to that of larger particle fluxes.

The detector package is mounted on the side of the spacecraft. The normal to the aperture is co-planar with the roll axis and the local radius through the package and tilted toward the Sun at a 45°

angle with the local radius.

Three FPA's are used to acquire data in coincidence and individual modes from each detector. The data are accumulated for 7.5 seconds so all eight discriminator settings are selected once a minute. At the beginning of every even frame the accumulated data are shifted from the three FPA's into storage registers, the FPA's are reset to zero, the next set of discriminator settings is selected, and data accumulation is begun again. Data in the storage registers are transmitted only in telemetry formats 1 and 2. The contents of a three bit counter are telemetered every 7.5 seconds to identify the discriminator settings in use.

A much more detailed description of this experiment is contained in "A Satellite Telescope for Protons and Alphas" by Paul R. Morel, Frederick A. Hanser, and Bach Sellers, AFCRL-TR-74-0531, November 1974.

Experiment 21, Low Energy Proton Spectrometer:

Experimenters: J.G. Kelley, L. Katz, G.K. Yates, Air Force Geophysical Laboratory, Bedford, Massachusets 01730

Two totally depleted silicon surface barrier detectors mounted in series form a sensor to measure the number of protons with energies between 150 kev and 6 Mev. Pulse height analysis of dE/dx in the front detector for particles which do not penetrate to the rear detector separates the proton counts into 11 energy channels. A twelfth channel counts the number of protons which penetrate to the rear detector. Approximate bounds of the twelve energy channels are as follows:

Channel	Mev	Channel	Mev
1	.10 - .14	7	.62 - .86
2	.14 - .17	8	.86 - 1.3
3	.17 - .23	9	1.3 - 1.8
4	.23 - .32	10	1.8 - 2.7
5	.32 - .45	11	2.7 - 6.0
6	.45 - .62	12	>6.0

Permanent magnets deflect incident electrons with energy less than 0.6 Mev. There is no rejection of counts generated by alpha particles or heavier nuclei, but their contribution is assumed small in comparison to that of protons.

The detector package is mounted on the side of the spacecraft. The normal to the aperture is co-planar with the roll axis and the local radius through the package and tilted toward the Sun at a 45° angle with the local radius.

Twelve FPA's are used to acquire data from the twelve channels. The data are accumulated for two minutes. At the beginning of each TMTC the FPA's are locked, their contents transferred to

storage registers for telemetering, reset to zero, and permitted to accumulate data again. Data in the storage registers are transmitted only in telemetry formats 1 and 2.

An Am 241 source automatically swings into a position to stimulate the detector for 4 seconds at intervals of approximately 6.5 hours. The counts from the source are superposed on the proton counts accumulated during the two minute sampling interval. A calibration warning analog monitor associated with the experiment changes from 0 volts to 5 volts ten minutes before the calibration source moves from its stowed position and holds the 5 volt level until the calibration source is moved into the field of view of the detector. The analog monitors are subcommutated so the calibration warning monitor is telemetered at 8 minute intervals.

A much more detailed description of this experiment is contained in "Design of a Low Energy Proton Spectrometer" by John Pantazis, Alan Huber, and M. Patricia Hagan, AFCRL-TR-75-0637, December 1975.

Experiment 22, Solar Flare Electrons:

Experimenter: A.L. Vampola, The Aerospace Corporation,
Los Angeles, California 90045

This experiment momentum analyzes incident electrons by means of uniform solenoidal magnetic fields produced by permanent magnets. Arrays of silicon detectors at the 180° primary focus detect the electrons. The electrons are sorted into 12 channels according to energy as follows:

Channel	Energy (kev)	Channel	Energy (kev)
1	12	7	334
2	35	8	592
3	65	9	856
4	105	10	1109
5	150	11	1354
6	130	12	1600

A thirteenth channel monitors penetrating protons with energy greater than 70 Mev.

The detector package is mounted on the side of the spacecraft. The normal to the aperture is perpendicular to the spacecraft's roll axis and parallel to the local radius. As the spacecraft rolls, the experiment sweeps a great circle.

Nineteen FPA's are used to acquire data from the thirteen channels. Nine of the channels - all except 1, 3, 7, and 8 - have a two minute accumulation period. At the beginning of each TMTC the nine FPA's associated with these channels are locked, their values shifted into storage registers for telemetering, reset to zero, and allowed to accumulate counts again. Data accumulated during a TMTC is telemetered during the next cycle. Channels 3 and 8 have a 15

second accumulation synchronized with the TMTC. The locking, shifting, resetting, and restarting sequence for the two FPA's associated with channels 3 and 8 occurs at the beginning of the TMTC and at 15 second intervals thereafter. Channels 1 and 7 have a two minute cycle, but actual data sampling is controlled by the satellite's roll reference system. As the satellite rolls, the roll reference system divides the great circle swept by the detector into 90° sectors. Channel 1 and 7 each have four FPA's. One FPA is associated with each 90° sector. At the beginning of each TMTC the eight FPA's associated with these channels are shifted and reset to zero. They are not allowed to accumulate data until a star pulse occurs. Then data from each 90° sector is shunted to its proper FPA for 27 complete rolls. The eight FPA's are then locked until the beginning of the next TMTC. Data acquired during one TMTC is transmitted during the next.

Transmission of data from the 13 channels occurs only when the satellite is using telemetry formats 1 and 2.

Experiment 23, Antisolar protons > 10 Mev:

Experimenter: J.B. Blake, The Aerospace Corporation,
Los Angeles, California 90045

This instrument is intended to detect protons and alpha particles heading toward the Sun. It is essentialy identical to experiment 14 except that it is mounted on the surface of the spacecraft which always faces away from the Sun.

Experiment 24, X-ray Background:

Experimenters: G.G. Fritz, R. Lucke, R.C. Henry, Code 4120,
Naval Research Laboratory

This experiment is the only experiment aboard SOLRAD 11 which did not produce data from at least one of the spacecraft. It was to use an ultrapure germanium detector to measure the galactic x-ray background radiation in the 0.5 to 20 kev (0.6 to 25 Å) range with an energy resolution of 0.3 kev. The desired resolution was to be obtained by cooling the detector to the 70° to 100° K range by passive means. Pulse height analyses of the detector output was to separate the pulses into 256 channels. The experiment was equipped with dual 256 channel memories so one could be accumulating data while the other was being read by the telemetry. The sampling period and the time required for a complete reading of a memory was 16 minutes.

The detector is mounted on the anti-solar surface of the spacecraft. As the satellite moved with the Earth around the Sun, the detector annually swept a great circle roughly paralleling the ecliptic. The field of view was either 20° or 3° full width at

half maximum depending on the position of a three-lobed wheel mounted in front of the detector's aperture. The three lobes were ninety degrees apart with a gap where a fourth lobe would be. One lobe limited the field of view to 3°. Another lobe contained an Fe 55 source for calibration. The third lobe was opaque to X-rays so the background response of the detector and electronics could be determined.

On SOLRAD 11A a protective cover over the experiment failed to move away from the sensor. On SOLRAD 11B the data were excessively noisy, possibly because the ultrapure germanium element became too hot during the ascent from synchronous to final orbital altitude. During this ascent the anti-solar surface of SOLRAD 11B was continuously pointed toward the Sun.

Experiment 25, Gamma Ray Burst Monitor:

Experimenters: W.D. Evans. R.W. Klebesadel, Los Alamos Scientific Laboratory, Los Alamos, New Mexico 87545
R.E. Spalding, Sandia Laboratories, Albuquerque, New Mexico 87115

A pair of detectors in each satellite observe gamma rays in the 0.2 to 2 Mev range. Each detector consists of a CsI scintillating crystal, a photomultiplier tube, a high voltage power supply, and amplifier circuits. Pulse height analysis resolves observed pulses into 0.2 - 0.3, 0.3 - 0.4, 0.4 - 0.6, and 0.6 - 2 Mev channels plus either a 0.2 - 2 or a 0.3 - 0.6 Mev channel. Each detector is capable of 4π steradians coverage, but each is occluded to some extent by surrounding satellite components. Therefore, the detectors are mounted 180° apart within each spacecraft to assure continuous 4π steradians coverage. Counts from the two detectors are combined and then analyzed to determine whether a gamma ray burst event is in progress.

Since gamma ray bursts are short lived and relatively infrequent, the experiment is usually monitoring the background counting rate. Samples are taken at 14.6 millisecond intervals. A 20 second average of the counting rate in either the 0.2 - 2 Mev or the 0.3 - 0.6 Mev channel establishes the background counting rate. Exceeding the background counting rate to approximately 7 sigma significance during a 625 millisecond period triggers storage of data in the experiment's memory. While waiting for a gamma ray burst to be identified, the experiment retains in a presample storage the most recent 60 samples, including those obtained during the 625 millisecond comparison period. When an event is identified these presamples are shifted into the experiment memory. The data samples are six-bit words. Each time a gamma ray event is identified 128 six-bit words are stored in the experiment memory as 64 twelve bit words. The 128 six-bit words include 8 words of auxiliary information, 60 words of presample data, and 60 words taken after the start of

the storage cycle. The 8 words of auxiliary information include time of event commencement from the experiment's clock, event identification, calibration mode, and identification of the 0.2 - 2 Mev or the 0.3 - 0.6 Mev channel as the selected channel for event trigger and background monitoring. The 60 presamples and the 60 event samples are stored as 5 groups of 12 samples each as follows: 8 samples of 0.2 - 2 Mev or 0.3 - 0.6 Mev data followed by 1 sample each of 0.2 - 0.3, 0.3 - 0.4, 0.4 - 0.6, and 0.6 - 2.0 Mev data. The numbers contained in the data samples can represent detector pulses or time. If the data sample has a value of 15 or less, it represents the number of detector pulses during a 14.6 millisecond sampling interval. If the number in the data sample is 16 through 63, it represents units of time (approximately 0.305 milliseconds) required to obtain 16 pulses from the detectors. The register counting time units is offset by 16 units so a count of time units can never be displayed as less than 16 and thereby fall into the range of values reserved for detector pulses. When the 60 event samples have been taken, the experiment logic will compare data obtained during the next 625 milliseconds with the pre-event background rate to see if the event is still in progress. If the event is over, the experiment reverts to monitoring the background counting rate. If the event is still in progress, the storage cycle is retriggered and another set of 128 six-bit samples is stored. Retriggering of the storage cycle can occur seven times. The experiment memory has a capacity for 1024 twelve-bit words and can thus accommodate 16 storage cycles. Therefore, a single event cannot use more than half of the memory's capacity. If the memory's capacity is exceeded, it starts writing over the oldest data. If the oldest data have not been telemetered prior to memory overflow, these oldest data are lost. Readout of the experiment's memory is only accomplished in telemetry format 2 at a rate of one word per frame. Complete readout of the 1024 word memory requires 64 minutes.

The value contained in the least significant four bits of the 6 bit event counter is transmitted at 7.5 second intervals in telemetry formats 1 and 2, and even more frequently in formats 4 and 5. A change in the event counter's value indicates triggering of storage cycles so the need for transmission of the memory can be recognized.

The gamma ray events primarily sought have origins outside the solar system. By making use of the difference in arrival time of the gamma ray event at two widely separated spacecraft, it is possible to define a circle on the celestial sphere on which the source of the event must lie. Therefore, it is necessary to identify the onset time of an event at each satellite with millisecond accuracy and resolution. The experiment has its own clock for this purpose. Four in-flight calibration modes artificially generate a burst of detector pulses to start the data storage cycle so its proper operation can be verified. Four calibration modes are available so that the artificial pulses can be generated at different rates. The experiment electronics controls sequencing through the

calibration modes. Each calibration mode causes the experiment clock value at the beginning of the first TMTC after the calibrate command has been received to be stored in the experiment's memory. The beginning time of a TMTC can be determined on the ground with one millisecond accuracy and this will provide the absolute time reference for the experiment clock. Use of the calibration capability causes data to be stored in the experiment's memory so the contents of the memory should be telemetered before commanding calibration.

OPERATING LIFETIME OF EXPERIMENT SENSORS

The experiments were initially turned on one by one over the period 24 March through 15 April 1976. Initially 48 out of the 50 experiments produced usable data. Experiment 24 was unable to make background x-ray measurements from either satellite. As time passed, experiments ceased producing usable data either through sudden failures such as the loss of SOLRAD 11A's telemetry in June 1977, or through gradual loss of sensitivity. The following table lists the date beyond which no data from a given experiment is usable.

Experiment No.	11A	11B
1	June 1977	December 1976
2	June 1977	December 1976
3	June 1977	September 1979
4	June 1977	October 1979
5	June 1977	October 1979
6	June 1977	October 1979
7	June 1977	October 1979
8	June 1977	December 1976
9	June 1977	December 1978
10	June 1977	October 1976
11	March 1977	December 1976
12	June 1977	October 1979
13	June 1977	October 1979
14	June 1977	December 1976

15	January 1977	February 1978
16	June 1977	December 1976
17	June 1977	December 1976
18,19	June 1977	December 1976
20	June 1977	December 1976
21	January 1977	November 1978
22	June 1977	December 1976
23	June 1977	December 1976
24	-----	-----
25	June 1977	December 1976

Since data from many experiments on SOLRAD 11 have not been carefully examined, there is no certainty that each experiment produced usable data right up to the date listed above. There is certainty that any data collected from an experiment after the date listed above is not usable. Also, many experiments suffered partial failures prior to the dates listed above, such as through failure of one or more sensors of a multi-sensor package or one or more channels of multi-channel experiments. The dates listed in the above table indicate the date after which it is certain that no channel or sensor in an experiment produced usable data.

DATA AVAILABILITY

All of the data from the SOLRAD 11 satellites received by the Blossom Point Satellite Tracking Facility, or by NASA ground stations and relayed to Blossom Point, have been recorded on magnetic tapes. These tapes have been edited to cull out obviously bad data, and are stored at NRL. Programs for NRL's DEC-10 computer are available to access data from any experiment for any time period.

ACKNOWLEDGEMENTS

We greatly appreciate the fine work performed by NRL's Space Systems Division in designing and constructing the SOLRAD 11 satellites. We are indebted to the personnel of the Blossom Point Satellite Tracking Facility for their vigilance in tending the spacecraft. We gratefully acknowledge NASA's extensive assistance with data acquisition. We appreciate the efforts of NRL's Space Environment Data Analysis

Center in processing, editing, and cataloging the huge amount of data telemetered. We compliment all of the experimenters on the high quality of the experiments which they delivered. We understand and appreciate the efforts required to deliver a good experiment.

A project as large as the SOLRAD Project required the efforts of many people - well over a hundred - to achieve its goals. It is impossible to list everyone, although we would like to. Certainly some names would be forgotten; but also certainly, there are some who contributed significantly to the satellites or experiments without our knowledge. Six people played such key roles in the construction of the SOLRAD 11 satellites that we must mention them by name: E.W. Peterkin, SOLRAD Project Manager; Jim Winkler, SOLRAD Spacecraft Manager; Andy Fox, Bob Palma, Larry Bowles, and Bob Grant, SOLRAD Satellite Coordinators. Our thanks to all.

REFERENCES

D. Baker, "Flare Classificaton Based upon X-ray Intensity", AIAA Paper 70-1370, Huntsville, Alabama (1970).

K.P. Dere, D.M. Horan, and R.W. Kreplin, J. Atmospheric Terrest. Phys. 36, 989 (1974).

R.F. Donnelly and J.H. Pope, "The 1-3000 Å Solar Flux for a Moderate Level of Solar Activity for Use in Modeling the Ionosphere and Upper Atmosphere", Tech. Rep. ERL 276-SEL 25, NOAA, Boulder, Colorado (1973).

W.G. Fastie, J. Optical Society of America 42, 641 (1952).

D.M. Horan and R.W. Kreplin, "The SOLRAD 10 Satellite, Explorer 44, 1971-058A", NRL Report 7408, July 1972.

D.M. Horan, R.W. Kreplin, K.P. Dere, and C.Y. Johnson, "SOLRAD 11 Experiment Timing, Telemetry and Command Summary", NRL Memorandum Report 3754, April 1978.

R.W. Kreplin, Ann. Geophys. 17, 151 (1961).

A.J. Lazarus, "Analysis of Solar Wind Data From the SOLRAD 11A and 11B Spacecraft", AFGL-TR-79-0056, February 1979.

J.F. Meekins, A.E. Unzicker, K.P. Dere, and R.W. Kreplin, "Absolute Calibraton of X-ray Ionization Chambers", NRL Report 7698, May 1974.

P.R. Morel, F.A. Hanser, and B. Sellers, "A Satellite Telescope for Protons and Alphas", AFCRL-TR-74-0531, November 1974.

J. Pantazis, A. Huber, M.P. Hagen, "Design of a Low Energy Proton Spectrometer", AFCRL-TR-75-0637, December 1975.

J.A.R. Samson, Techniques of Vacuum Ultraviolet Spectroscopy, Wiley, New York, 1967.

APPENDIX

Written and Oral Presentations of Research Results Based on SOLRAD 11 Data

Fritz, G.G. and Horan, D.M., "Hard X-ray Emission from a Recent Gamma Ray Burst", American Physical Society Meeting, Washington, D.C., 1977.

Horan, D.M. and Kreplin, R.W., "Soft X-ray Emission from the Non-Flaring Sun as a Precursor to Flare Activity", Solar-Terrestrial Predictions Proceedings, Vol. 3: Solar Activity Predictions. Edited by R.F. Donnelly, NOAA, Boulder, Colorado, March 1980.

Horan, D.M. and Kreplin, R.W., "Measurements of Solar EUV and Soft X-ray Emission During Sudden Frequency Deviations", Journal of Geophysical Research, Vol. 85, No. A8, pp. 4257-4269, 1 August 1980.

Horan, D.M. and Kreplin, R.W., "Simultaneous Measurements of EUV and Soft X-ray Flare Emission", XIVth ESLAB Symposium on Physics of Solar Variations, Scheveningen, The Netherlands, September, 1980.

Horan, D.M. and Kreplin, R.W., "Simultaneous Measurements of EUV and Soft X-ray Flare Emission", Solar Physics, 74, pp. 265-272, 1981.

Horan, D.M., Kreplin, R.W. and Dere, K.P., "Direct Measurements of Gradual Extreme Ultraviolet Emission from Large Solar Flares". Submitted to Solar Physics, June 1982.

Horan, D.M., Kreplin, R.W. and Fritz, G.G., "Measurements of Impulsive EUV and Hard X-ray Solar Flare Emission", American Astronomical Society Meeting, College Park, Maryland, June 1980.

Horan, D.M., Kreplin, R.W. and Fritz, G.G., "Direct Measurements of Impulsive EUV and Hard X-ray Solar Flare Emission", Astrophysical Journal, 255, April 1982.

Horan, D.M., Kreplin, R.W., Fritz, G.G. and Dere, K.P., "Direct Measurements of Gradual Extreme Ultraviolet Emission from Solar Flares", American Geophysical Union Meeting, Philadelphia, Pennsylvania, May 1982.

Kreplin, R.W., "Solar X-ray Radiation in the Current Solar Cycle", Atmosphere Explorer Symposium #2, Bryce Mts., Bayse, Virginia, October 1978.

Kreplin, R.W. and Horan, D.M., "Ionospheric Disturbance Forecasting Through Use of X-ray and EUV Measurements from the NRL SOLRAD Satellite", AGARD Symposium on Operational Modeling of the Aerospace Propagation Environment, April 1978; also, AGARD Conference Proceedings No. 238. Edited by H. Soicher, pp. 28.1-28.14, 1978.

Kreplin, R.W. and Horan, D.M., "Variability of Solar EUV in the Rise Phase of the Current Solar Cycle", XIVth ESLAB Symposium on Physics of Solar Variations, Scheveningen, The Netherlands, September 1980.

Kreplin, R.W. and Horan, D.M., "Solar X-ray Irradiance in Solar Cycle 21", IAGA Symposium, Edinburgh, Scotland, August 1981; also EGS Symposium, Uppsala, Sweden, August 1981.

Kreplin, R.W. and Horan, D.M., "Solar EUV Irradiance for the Period 3/76 Through 10/79", American Geophysical Union Meeting, San Francisco, California, December 1981.

Kreplin, R.W. and Horan, D.M., "Solar Cycle Variability of EUV Emission Below 1000 Å", Fifth International Symposium on Solar-Terrestrial Physics, COSPAR Meeting, Ottawa, Canada, May 1982.

Kreplin, R.W., Horan, D.M. and Taylor, R.G., "Flare EUV Emission and Related Ionospheric Effects", International Symposium on Solar-Terrestrial Physics, COSPAR Meeting, Innsbruck, Austria, 1978.

Kreplin, R.W., Horan, D.M. and Taylor, R.G., "Measured Variation in Solar EUV Emission", American Astronomical Society Meeting, College Park, Maryland, June 1980.

Landini, M. and Monsignori Fossi, B.C., "X-ray Flaring Region Observed by Means of SOLRAD 11B Experiments", COSPAR Meeting, Tel Aviv, Israel, 1977.

Laros, J.G., Evans, W.D., Klebesadel, R.W., Olson, R.A. and Spalding, R.E., "Preliminary Results from SOLRAD 11 Gamma Burst Detectors", Nature, Vol. 267, No. 5607, pp. 131-132, 12 May 1977.

Mariska, John T. and Oran, Elaine S., "The E and F Region Ionospheric Response to Solar Flares: 1. Effects of Approximations of Solar Flare EUV Fluxes", Journal of Geophysical Research, Vol. 86, No. A7, pp. 5868-5872, 1 July 1981.

Oran, Elaine S. and Mariska, John T., "The Ionospheric Response to Solar Flares: I. Effects of Approximations of Solar Flare EUV Fluxes", NRL Memorandum Report 4428, 16 January 1981.

Weller, C.S., "The Near Earth Ultraviolet Environment", Proceedings of the Society of Photo-Optical Instrumentation Engineers, Vol. 279, pp. 216-222, 1981.

Weller, C.S., "SOLRAD 11 Observations of the 1220-1500 Å Far - UV Background Near the Galactic Poles", Bull. Am. Astron. Soc., Vol. 13, p. 537 ff., 1981.

Weller, C.S., "SOLRAD 11 Observations of the Far Ultraviolet Background". Submitted to The Astrophysical Journal, May 1982.

Weller, C.S. and Meier, R.R., "Characteristics of the Helium Component of the Local Interstellar Medium", Astrophysical Journal, Vol. 246, pp. 386-393, June 1981; also, Bull. Am. Astron. Soc., Vol. 11, p 684 ff., 1979.

END

FILMED

2-83

DTIC